AD-A052 583 ARMY ARMAMENT RESEARCH AND DEVELOPMENT COMMAND DOVER--ETC F/G 20/11
ISOPARAMETRIC ELEMENTS AS SINGULAR ELEMENTS FOR CRACK PROBLEMS.(U)
NOV 77 M A HUSSAIN, W E LORENSEN

UNCLASSIFIED ARLCB-TR-77041 SBIE-AD-E400 119 NL

| OF |
ADA
052583

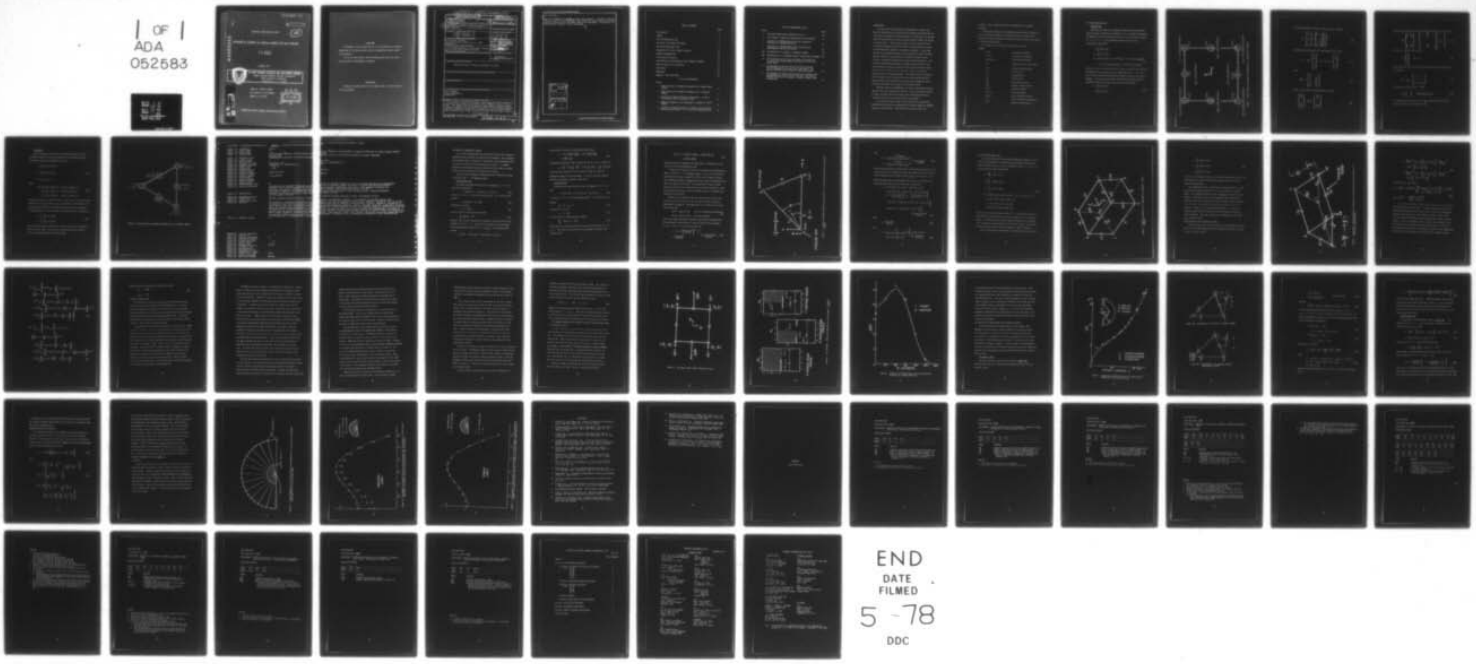

END
DATE FILMED
5-78
DDC

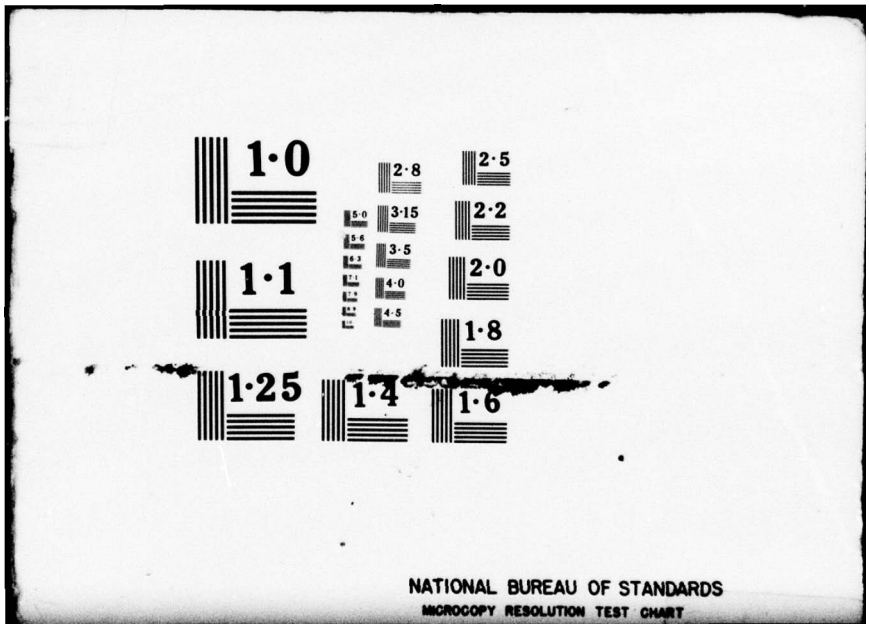
1·0
1·1
1·25
1·4
1·6
1·8
2·0
2·2
2·5
2·8
3·15
3·5
4·0
4·5
5·0
NATIONAL BUREAU OF STANDARDS
MICROCOPY RESOLUTION TEST CHART

AD

TECHNICAL REPORT ARLCB-TR-77041

(12)

ISOPARAMETRIC ELEMENTS AS SINGULAR ELEMENTS FOR CRACK PROBLEMS

M. A. Hussain
W. E. Lorensen

November 1977

US ARMY ARMAMENT RESEARCH AND DEVELOPMENT COMMAND
LARGE CALIBER WEAPON SYSTEMS LABORATORY
BENÉT WEAPONS LABORATORY
WATERVLIET, N. Y. 12189

AMCMS No. 611102.11.H4500
DA Project No. 1L161102AH45
PRON No. EJ-7-Y0011

APPROVED FOR PUBLIC RELEASE; DISTRIBUTION UNLIMITED

DISCLAIMER

The findings in this report are not to be construed as an official Department of the Army position unless so designated by other authorized documents.

The use of trade name(s) and/or manufacturer(s) does not constitute an official indorsement or approval.

DISPOSITION

Destroy this report when it is no longer needed. Do not return it to the originator.

(18) SBIE (19) AD-E400 119

SECURITY CLASSIFICATION OF THIS PAGE (When Data Entered)

REPORT DOCUMENTATION PAGE

READ INSTRUCTIONS BEFORE COMPLETING FORM

1. REPORT NUMBER (14) ARLCB-TR-77041	2. GOVT ACCESSION NO. (9)
3. RECIPIENT'S CATALOG NUMBER: Technical rept.	
4. TITLE (and Subtitle) (6) ISOPARAMETRIC ELEMENTS AS SINGULAR ELEMENTS FOR CRACK PROBLEMS.	5. TYPE OF REPORT & PERIOD COVERED
	6. PERFORMING ORG. REPORT NUMBER
7. AUTHOR(s) (10) M. A. Hussain, W. E. Lorensen	8. CONTRACT OR GRANT NUMBER(s) (12) 57p.
9. PERFORMING ORGANIZATION NAME AND ADDRESS Benet Weapons Laboratory Watervliet Arsenal, Watervliet, N.Y. 12189 DRDAR-LCB-TL	10. PROGRAM ELEMENT, PROJECT, TASK AREA & WORK UNIT NUMBERS AMCMS No. 611102.11.H4500 DA Proj. No. (16) 1L161102AH45 PRON No. EJ-7-Y0011
11. CONTROLLING OFFICE NAME AND ADDRESS US Army Armament Research and Development Command Large Caliber Weapon System Laboratory Dover, New Jersey 07801	12. REPORT DATE (11) Nov [redacted]77 13. NUMBER OF PAGES 56
14. MONITORING AGENCY NAME & ADDRESS (if different from Controlling Office)	15. SECURITY CLASS. (of this report) UNCLASSIFIED 15a. DECLASSIFICATION/DOWNGRADING SCHEDULE

16. DISTRIBUTION STATEMENT (of this Report)

Approved for public release; distribution unlimited.

17. DISTRIBUTION STATEMENT (of the abstract entered in Block 20, if different from Report)

18. SUPPLEMENTARY NOTES

19. KEY WORDS (Continue on reverse side if necessary and identify by block number)

Finite Elements
Fracture (Mechanics)
Isoparametric

20. ABSTRACT (Continue on reverse side if necessary and identify by block number)

The quadratic isoparametric elements, which embody the inverse square root singularity, are used for calculating the stress intensity factors at tips of cracks. The elements used are the quadratic quadrilateral (8-node), quadratic triangular (6-node) and three-dimensional quadratic "brick" (20-node) elements. Singularity elements are obtained in a simple manner by placing the mid-side nodes at quarter points in the vicinity of the crack tip or an edge. These ele-

(see reverse side)

DD FORM 1 JAN 73 1473 EDITION OF 1 NOV 65 IS OBSOLETE

410 163

SECURITY CLASSIFICATION OF THIS PAGE (When Data Entered)

Block 20 (cont)

ments are implemented in NASTRAN as dummy (user) elements. The method eliminates the use of special crack tip elements and in addition, these elements satisfy the constant strain and rigid body modes required for convergence. The stability of two-dimensional elements is also investigated.

TABLE OF CONTENTS

LIST OF ILLUSTRATIONS

LIST OF ILLUSTRATIONS (cont)

INTRODUCTION

In "Crack Tip Finite Elements are Unnecessary", Henshell and Shaw [1] reported that the inverse of the Jacobian associated with the coordinate transformation becomes singular at a point when the mid-side nodes for two-dimensional eight-node quadrilateral elements are placed at quarter points. Interestingly enough, the same singularity was discovered independently by Barsoum [2] for two-dimensional, as well as three-dimensional quadratic isoparametric elements. It was then natural to investigate the order of the singularity; and it was found that the singularity was precisely of the order one-half for the strains, a phenomenon encountered in linear fracture mechanics. This remarkable phenomenon completely eliminates the necessity of incorporating special crack-tip elements [3,4,5] and has additional advantages over the special crack-tip elements; namely, it satisfies constant strain and rigid body modes. The special crack-tip elements were introduced in the literature to avoid the extremely fine grid mesh required in the vicinity of the crack and the cumbersome extrapolation needed when using regular finite elements [6,7].

Advanced versions of NASTRAN [8], as well as some general purpose programs have such isoparametric elements. Hence, by judicious choice of nodes, accurate crack-tip elements can be formulated and stress intensity factors for cracks and flaws can be computed.

In the present report, after a brief review of the theoretical formulation, we discuss the implementation of these elements as NASTRAN dummy user elements [18]. Test problems are done to assess the

accuracy. Stress intensity factors are computed for a C-shaped specimen.

Finally the stability of two-dimensional quadrilateral element as well as triangular element is investigated; and it is shown that a triangular element preserves the required singularity under perturbation of the mid-side node. [19]

The method can be extended to higher order elements.

SYMBOLS

(x,y)	Cartesian coordinates
(ξ,η)	Curvilinear coordinates
x_i, y_i, ξ_i, η_i	Grid point coordinates
N_i	Shape function at grid point i
u,v	Cartesian displacements
$\{\varepsilon\}$	Strain vector
$[J]$	Jacobian matrix
$\{\sigma\}$	Stress vector
$[D]$	Stress-strain matrix
$[K]$	Element stiffness matrix
E,G,ν	Elastic constants
L_1, L_2, L_3	Area coordinates
K_I, K_{II}	Stress intensity factors
r,θ	Local cylindrical coordinates
$\{F\}^e$	Equivalent nodal forces

THE TWO-DIMENSIONAL CASE

QUADRILATERAL

Following the notation of Zienkiewicz [9] the eight node quadrilateral element in Cartesian coordinates (x,y) is formulated by mapping its geometry into the curvilinear space (ξ,η) of the normalized square $(-1 \leq \xi \leq 1,\ -1 \leq \eta \leq 1)$ by quadratic shape functions of the 'Serendipity' family [9]:

$$x = \sum_{i=1}^{8} N_i(\xi,\eta)x_i \ ,$$

$$y = \sum_{i=1}^{8} N_i(\xi,\eta)y_i \ ,$$

$$N_i = [(1+\xi\xi_i)(1+\eta\eta_i) - (1-\xi^2)(1+\eta\eta_i) - (1-\eta^2)(1+\xi\xi_i)]\xi_i^2\eta_i^2/4 \qquad (1)$$

$$+ (1-\xi^2)(1+\eta\eta_i)(1-\xi_i^2)\eta_i^2/2 + (1-\eta^2)(1+\xi\xi_i)(1-\eta_i^2)\xi_i^2/2,$$

where N_i is the shape function at node i whose Cartesian and curvilinear coordinates are (x_i,y_i) and (ξ_i,η_i) respectively, (i=1 ... 8). The details of the shape functions and the numbering sequence are given in Figure 1. The same shape functions are used to interpolate the displacements within the element, hence the name isoparametric.

$$u = \sum_{i=1}^{8} N_i(\xi,\eta)u_i \ ,$$

$$v = \sum_{i=1}^{8} N_i(\xi,\eta)v_i \ . \qquad (2)$$

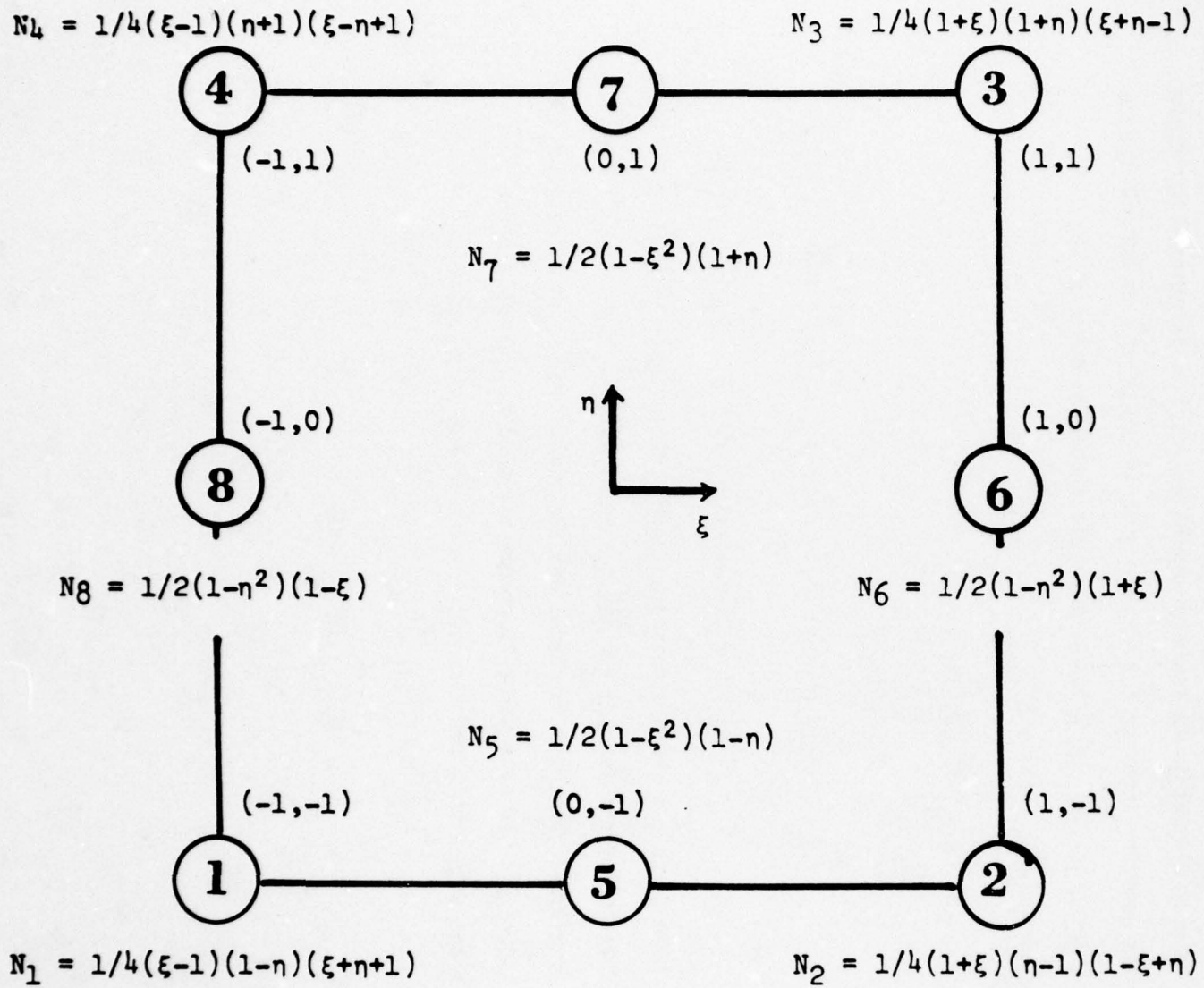

Figure 1. Shape functions and numbering sequence for a quadrilateral element.

The stiffness matrix is found in the usual way as follows:

$$\{\varepsilon\} = \begin{Bmatrix} \varepsilon_x \\ \varepsilon_y \\ \gamma_{xy} \end{Bmatrix} = \begin{bmatrix} \frac{\partial}{\partial x} & 0 \\ 0 & \frac{\partial}{\partial y} \\ \frac{\partial}{\partial y} & \frac{\partial}{\partial x} \end{bmatrix} \begin{Bmatrix} u \\ v \end{Bmatrix} . \tag{3}$$

Substituting from Equation (2) into Equation (3) we have:

$$\{\varepsilon\} = [B] \begin{Bmatrix} \vdots \\ u_i \\ \\ v_i \\ \vdots \end{Bmatrix} = [\ldots\ B_i\ \ldots] \begin{Bmatrix} \vdots \\ u_i \\ \\ v_i \\ \vdots \end{Bmatrix} \tag{4}$$

where

$$[B_i] = \begin{bmatrix} \frac{\partial N_i}{\partial x} & 0 \\ 0 & \frac{\partial N_i}{\partial y} \\ \frac{\partial N_i}{\partial y} & \frac{\partial N_i}{\partial x} \end{bmatrix} \tag{5}$$

By the rules of partial differentiation we obtain

$$\begin{Bmatrix} \frac{\partial N_i}{\partial x} \\ \\ \frac{\partial N_i}{\partial y} \end{Bmatrix} = [J]^{-1} \begin{Bmatrix} \frac{\partial N_i}{\partial \xi} \\ \\ \frac{\partial N_i}{\partial \eta} \end{Bmatrix} \tag{6}$$

where [J], the Jacobian matrix, by virtue of Equation (1) is given by

$$[J] = \begin{bmatrix} \frac{\partial x}{\partial \xi} & \frac{\partial y}{\partial \xi} \\ \\ \frac{\partial x}{\partial \eta} & \frac{\partial y}{\partial \eta} \end{bmatrix} = \begin{bmatrix} \cdots & \frac{\partial N_i}{\partial \xi} & \cdots \\ \\ \cdots & \frac{\partial N_i}{\partial \eta} & \cdots \end{bmatrix} \begin{bmatrix} \cdot & \cdot \\ \cdot & \cdot \\ x_i & y_i \\ \cdot & \cdot \\ \cdot & \cdot \end{bmatrix} . \qquad (7)$$

The stress components are given by

$$\{\sigma\} = \begin{Bmatrix} \sigma_x \\ \sigma_y \\ \tau_{xy} \end{Bmatrix} = [D] \quad \{\varepsilon\} \qquad (8)$$

where [D] is the stress-strain matrix and for the case of plane stress is given by

$$[D] = \frac{E}{1-\nu^2} \begin{bmatrix} 1 & \nu & 0 \\ \nu & 1 & 0 \\ 0 & 0 & (1-\nu)/2 \end{bmatrix} . \qquad (9)$$

The element stiffness matrix is then:

$$[K] = \int_{-1}^{1} \int_{-1}^{1} [B]^T[D][B]\det|J|d\xi d\eta \ . \qquad (10)$$

The integration in Equation (10) is done numerically by nine-point Gaussian quadrature as explained in [9].

TRIANGULAR

Again, following the notation of Zienkiewicz [9] the six node triangular element in cartesian coordinates is formulated by transformations using area coordinates (L_1, L_2, L_3):

$$x = \sum_{i=1}^{6} N_i(L_1, L_2, L_3)x_i \ ,$$

$$y = \sum_{i=1}^{6} N_i(L_1, L_2, L_3)y_i \ , \tag{11}$$

$$L_1 + L_2 + L_3 = 1,$$

where

$$\begin{aligned} N_i = {} & L_i L_{1i}(2L_1 - 1)(2L_{1i} - 1) - 16L_1 L_2 L_{1i} L_{2i}(2L_{3i} - 1) \\ & + L_2 L_{2i}(2L_2 - 1)(2L_{2i} - 1) - 16L_2 L_3 L_{2i} L_{3i}(2L_{1i} - 1) \\ & + L_3 L_{3i}(2L_3 - 1)(2L_{3i} - 1) - 16L_3 L_1 L_{3i} L_{1i}(2L_{2i} - 1) \ , \end{aligned} \tag{12}$$

Equation (12) gives the shape function at node i whose cartesian and area coordinates are (x_i, y_i) and (L_{1i}, L_{2i}, L_{3i}) respectively. The details of the shape function (12) and the numbering sequence are given in Figure 2. The displacements for the isoparametric triangular element are given by:

$$\begin{aligned} u &= \sum_{i=1}^{6} N_i(L_1, L_2, L_3)u_i \ , \\ v &= \sum_{i=1}^{6} N_i(L_1, L_2, L_3)v_i \ . \end{aligned} \tag{13}$$

The rest of the analysis proceeds in a similar way as for the quadrilateral case given above. The numerical integration for the stiffness matrix is done using Hammer's Quadrature [9].

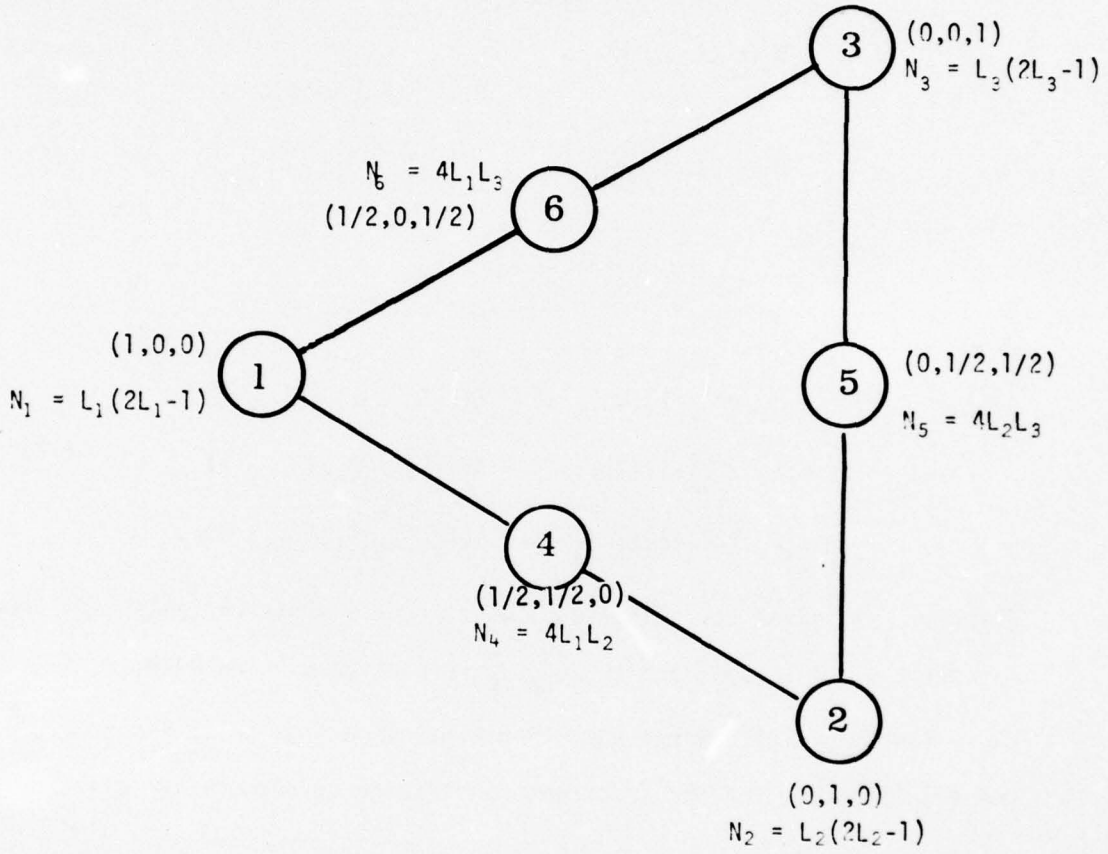

Figure 2. Shape functions and numbering sequence for a triangular element.

AD NUMBER	••••••••••••••••••••••••	E400119 ••••••••••••••••••••,•••SCN--
FIELD 2:	FLD/GRP(S)	20110
FIELD 3:	ENTRY CLASS	U
FIELD 4:	NTIS PRICES	HC MF
FIELD 5:	SOURCE NAME	ARMY ARMAMENT RESEARCH AND DEVELOPMENT COM SYSTEMS LAB•
FIELD 6:	UNCLASS• TITLE	ISOPARAMETRIC ELEMENTS AS SINGULAR ELEMENT
FIELD 7:	CLASS• TITLE	
FIELD 8:	TITLE CLASS•	U
FIELD 9:	DESCRIPTIVE NOTE	TECHNICAL REPT•,
FIELD 10:	PERSONAL AUTHORS	HUSSAIN,M• A• ;LORENSEN,W• E• ;
FIELD 11:	REPORT DATE	NOV 77
FIELD 12:	PAGINATION	54P
FIELD 13:	SOURCE ACRONYM	
FIELD 14:	REPORT NUMBER	ARLCB-TR-77041
FIELD 15:	CONTRACT NUMBER	
FIELD 16:	PROJECT NUMBER	1L161102AH45
FIELD 17:	TASK NUMBER	
FIELD 18:	MONITOR SOURCE	
FIELD 19:	MONITOR SERIES	
FIELD 20:	REPORT CLASS	U
FIELD 21:	SUPPLEMENTARY NOTE	
FIELD 22:	ALPHA LIMITATIONS	DISTRIBUTION OF DOCUMENT CONTROLLED BY ARM COMMAND, ATTN: DRDAR-TSS, DOVER, NJ 07801• FROM DDC• CATALOGING INFORMATION SUPPLIED DEVELOPMENT COMMAND, ATTN: DRDAR-TSS, DOVE
FIELD 23:	DESCRIPTORS	•CRACKS, •CRACKING(FRACTURING), •FRACTURE(FINITE ELEMENT ANALYSIS
FIELD 24:	DESCRIPTOR CLASS•	U
FIELD 25:	IDENTIFIERS	NASTRAN COMPUTER PROGRAM, PE61102A, ASH45,
FIELD 26:	IDENTIFIER CLASS•	U
FIELD 27:	ABSTRACT	THE QUADRATIC ISOPARAMETRIC ELEMENTS, WHIC SINGULARITY, ARE USED FOR CALCULATING THE THE ELEMENTS USED ARE THE QUADRATIC QUADRI NODE) AND THREE-DIMENSIONAL QUADRATIC 'BRI ARE OBTAINED IN A SIMPLE MANNER BY PLACING VICINITY OF THE CRACK TIP OR AN EDGE• THES DUMMY (USER) ELEMENTS• THE METHOD ELIMINAT IN ADDITION, THESE ELEMENTS SATISFY THE CO FOR CONVERGENCE• THE STABILITY OF TWO-DIME
FIELD 28:	ABSTRACT CLASS•	U
▫		
FIELD 29:	INITIAL INVENTORY	0
FIELD 30:	ANNOTATION	
FIELD 31:	SPECIAL INDICATOR	@
FIELD 32:	REGRADING CATEGORY	
FIELD 33:	LIMITATION CODES	1 21
FIELD 34:	SOURCE SERIAL	
FIELD 35:	SOURCE CODE	393472
FIELD 36:	DOCUMENT LOCATION	7
FIELD 37:	CLASSIFIED BY	
FIELD 38:	DECLASSIFIED ON	
FIELD 39:	DOWNGRADED TO CONF•	
FIELD 40:	GEOPOLITICAL CODE	3628
FIELD 41:	SOURCE TYPE CODE	A
FIELD 42:	TAB ISSUE NUMBER	@@--@@

0119 ••••••••••••••••••••,••••SCN-- AJL06J

MF
ARMAMENT RESEARCH AND DEVELOPMENT COMMAND WATERVLIET NY LARGE CALIBER WEAPON
HS LAB.
RAMETRIC ELEMENTS AS SINGULAR ELEMENTS FOR CRACK PROBLEMS.

ICAL REPT.,
IN,M. A. ;LORENSEN,W. E. ;
V 77
P

-TR-77041

102AH45

IBUTION OF DOCUMENT CONTROLLED BY ARMY ARMAMENT RESEARCH AND DEVELOPMENT
ND, ATTN: DRDAR-TSS, DOVER, NJ 07801. THIS DOCUMENT IS NOT AVAILABLE
DDC. CATALOGING INFORMATION SUPPLIED BY ARMY ARMAMENT RESEARCH AND
OPMENT COMMAND, ATTN: DRDAR-TSS, DOVER, NJ 07801.
KS, *CRACKING(FRACTURING), *FRACTURE(MECHANICS), COMPUTER PROGRAMS,
E ELEMENT ANALYSIS

AN COMPUTER PROGRAM, PE611O2A, ASH45, LPN-PRON-EJ-7-Y0011

UADRATIC ISOPARAMETRIC ELEMENTS, WHICH EMBODY THE INVERSE SQUARE ROOT
LARITY, ARE USED FOR CALCULATING THE STRESS INTENSITY FACTORS AT TIPS OF CRACKS.
LEMENTS USED ARE THE QUADRATIC QUADRILATERAL (8-NODE), QUADRATIC TRIANGULAR (6
AND THREE-DIMENSIONAL QUADRATIC 'BRICK' (20-NODE) ELEMENTS. SINGULARITY ELEMENTS
BTAINED IN A SIMPLE MANNER BY PLACING THE MID-SIDE NODES AT QUARTER POINTS IN THE
ITY OF THE CRACK TIP OR AN EDGE. THESE ELEMENTS ARE IMPLEMENTED IN NASTRAN AS
(USER) ELEMENTS. THE METHOD ELIMINATED THE USE OF SPECIAL CRACK TIP ELEMENTS AND
DITION, THESE ELEMENTS SATISFY THE CONSTANT STRAIN AND RIGID BODY MODES REQUIRED
ONVERGENCE. THE STABILITY OF TWO-DIMENSIONAL ELEMENTS IS ALSO INVESTIGATED.

2

THE CRACK TIP SINGULARITY ELEMENT

It is clear from Equations (4) and (6) that we need the inverse of Jacobian matrix [J] before the strains can be computed. Hence, whenever the inverse of [J] is singular or, equivalently, the determinant of [J] is zero, the strains and stresses may become singular. A singular Jacobian is achieved by placing the adjacent mid-side nodes at quarter points from the node where the singularity is desired.

This will be illustrated by investigating the singularity at node 1 along the line 1 - 2 of Figures 1 and 2.

QUADRILATERAL CASE

Evaluating the shape functions given in Figure 1 at $\eta = -1$, we have the transformation

$$x = -1/2\xi(1-\xi)x_1 + 1/2\xi(1+\xi)x_2 + (1-\xi^2)x_5 \ . \qquad (14)$$

Choosing $x_1 = 0$, $x_2 = L$ and the quarter point $x_5 = L/4$, Equation (14) becomes

$$x = 1/2\xi(1+\xi)L + (1-\xi^2)L/4 \qquad (15)$$

Solving for ξ we have

$$\xi = -1 + 2\sqrt{x/L} \ . \qquad (16)$$

In this case the reduced Jacobian becomes

$$\frac{\partial x}{\partial \xi} = \frac{L}{2}(1+\xi) = \sqrt{xL} \ . \qquad (17)$$

Equation (17) clearly indicates the singularity for the inverse of the Jacobian at $x = 0$, $\xi = -1$. The order of singularity can be obtained from the displacement along line 1 - 2 (Fig. 1). From Equation (2) we have

$$u(\xi,-1) = -1/2\xi(1-\xi)u_1 + 1/2\xi(1+\xi)u_2 + (1-\xi^2)u_5 \ ,$$

and writing in terms of x from Equation (16) we have

$$u = -1/2(-1+2\frac{\sqrt{x}}{\sqrt{L}})(2-2\frac{\sqrt{x}}{\sqrt{L}})u_1 + 1/2(-1+2\frac{\sqrt{x}}{\sqrt{L}})(2\frac{\sqrt{x}}{\sqrt{L}})u_2 + 4(\frac{\sqrt{x}}{\sqrt{L}} - \frac{x}{L})u_5 \quad . \tag{18}$$

Differentiating Equation (18) we obtain the strains in the x-direction:

$$\varepsilon_x = \frac{\partial u}{\partial x} = -1/2[\frac{3}{\sqrt{xL}} - \frac{4}{L}]u_1 + 1/2[-\frac{1}{\sqrt{xL}} + \frac{4}{L}]u_2 + [\frac{2}{\sqrt{xL}} - \frac{4}{L}]u_5 \tag{19}$$

indicating the singularity of order one-half ($\frac{1}{\sqrt{x}}$), precisely the singularity needed for crack problems. It can be seen that Equation (19) also incorporates constant strain terms.

TRIANGULAR CASE

Evaluating the shape functions given in Figure 2 at $L_3 = 0$, we have

$$x = L_1(2L_1-1)x_1 + (1-L_1)(1-2L_1)x_2 + 4L_1(1-L_1)x_3 \tag{20}$$

choosing $x_1 = 0$, $x_2 = A$ and the quarter point $x_4 = A/4$, Equation (20) becomes

$$x/A = L_1^2 - 2L_1 + 1 \tag{21}$$

Solving for L_1 we have

$$L_1 = 1 - \sqrt{x/A} \tag{22}$$

For this case the reduced Jacobian becomes

$$\frac{\partial x}{\partial L_1} = 2A(L_1-1) = -2\sqrt{Ax} \tag{23}$$

which shows the singularity for the inverse of the Jacobian at $x = 0$, $L_1 = 1$. The order of singularity can be obtained, as before, from Equation (13).

$$u(L_3=0) = (1-\sqrt{x/A})(1-2\sqrt{x/A})u_1 + \sqrt{x/A}(2\sqrt{x/A}-1)u_2 + 4\sqrt{x/A}(1-\sqrt{x/A})u_3 \quad (24)$$

The above expression indicates the same order of singularity for the strains as for the quadrilateral case.

In both of the above cases we have investigated the singularity at Node 1 along line 1 - 2 of Figures 1 and 2. However, for the case of quadrilateral element, as opposed to the case of triangular element, the singularity at Node 1 (Figure 1) along any other ray emanating from Node 1 is weaker than one-half. The singularity of order one-half along any other ray can be achieved by collapsing grid points 1, 4 and 8 and placing grid points 5 and 7 at quarter points in cartesian coordinates from grid point 1.

Without loss of generality let the cartesian map of such a collapsed quadrilateral element as well as the triangular element be represented in Figure 3. Using Equations (7), (1) and (11) it can be easily shown that

$$\det|J| = \frac{1}{16}(1+\xi)^3\sin\alpha \quad \text{(for the collapsed quadrilateral)}$$
$$\det|J| = 2(L_2+L_3)^2\sin\alpha \quad \text{(for the triangle)} \quad (25)$$

Both of the above expressions vanish at grid point (1) along any ray. The coordinate transformations in terms of cylindrical coordinates $r, \theta (x = r\cos\theta, y = r\sin\theta)$, are given by:

$$\xi = -1 + 2\left\{\frac{\cos(\theta-\alpha/2)}{\cos\alpha/2}\right\}^{1/2} r^{1/2}$$
$$\eta = \frac{\tan(\theta-\alpha/2)}{\tan(\alpha/2)} \quad \text{(For Quadrilateral Element)} \quad (26)$$

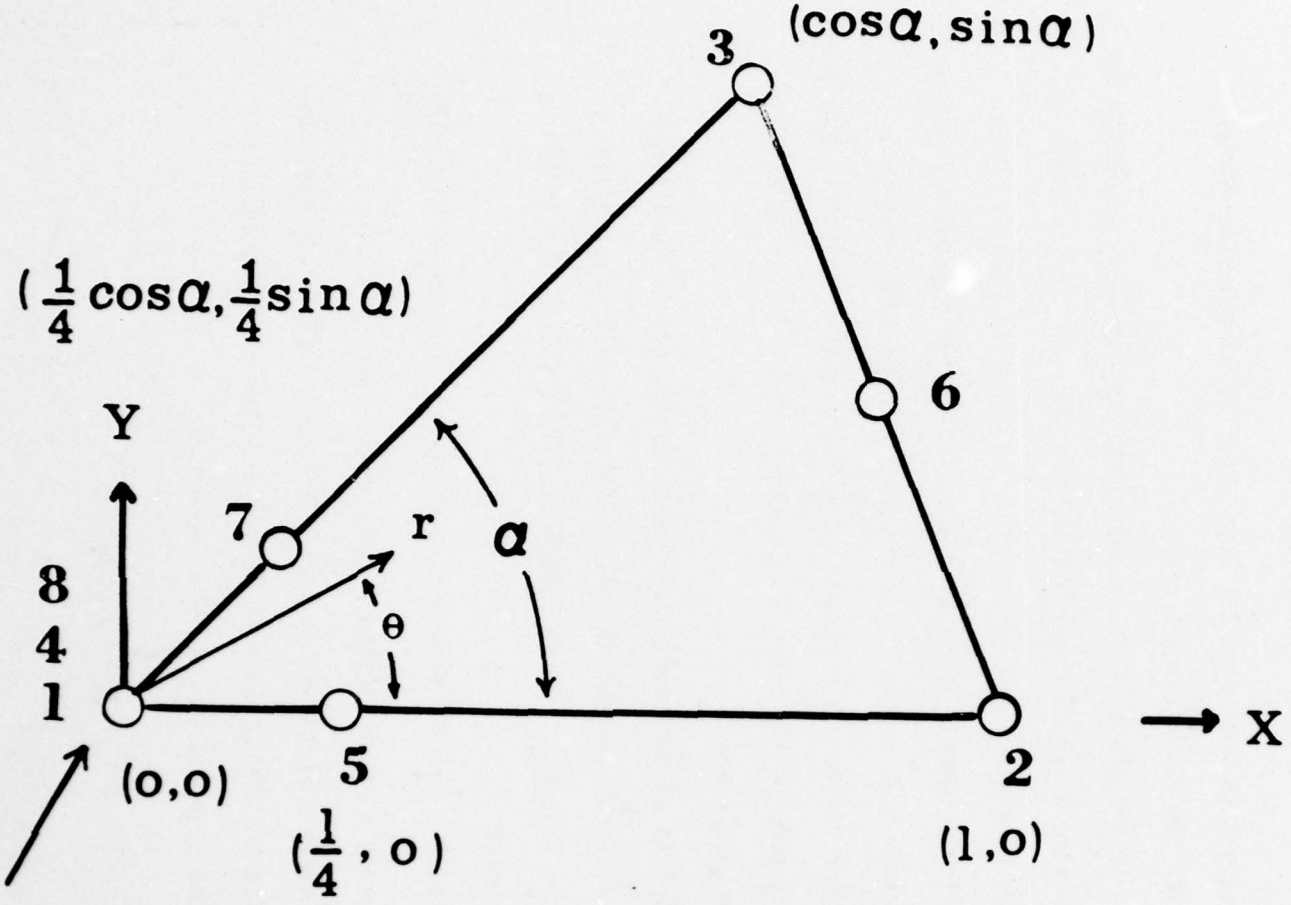

Figure 3. Singularity element obtained by collapsing 1, 4, and 8 and placing 5 and 7 at quarter points.

and

$$L_2 = \frac{r^{1/2}\sin(\alpha-\theta)}{\{2\sin\alpha\ \sin\alpha/2\ \cos(\theta-\alpha/2)\}^{1/2}}$$

$$L_3 = \frac{r^{1/2}\sin\theta}{\{2\sin\alpha\ \sin\alpha/2\ \cos(\theta-\alpha/2)\}^{1/2}} \quad \text{(For Triangular Elements)} \tag{27}$$

When these expressions are substituted in Equations (2) and (13), it is easily seen that the displacements have the proper behavior to insure a strain singularity of the order one-half ($\frac{1}{\sqrt{r}}$) at the crack tip. (It should be noted that the displacements for nodes 1, 4, and 8 of the collapsed quadrilateral must be the same.) Explicitly,

$$\begin{aligned} u &= \{1+\xi\}[-1/4(1-\eta)(1-\xi+\eta)u_2 + 1/4(1+\eta)(\xi+\eta-1)u_2 \\ &\quad + 1/2(1-\xi)(1-\eta)u_5 + 1/2(1-\eta^2)u_6 + 1/2(1-\xi)(1+\eta)u_7] \\ &= 2r^{1/2}\frac{\cos^{1/2}(\theta-\alpha/2)}{\cos^{1/2}(\alpha/2)}\Bigg[2(1 - \frac{\cos^{1/2}(\theta-\alpha/2)}{\cos^{1/2}(\alpha/2)}r^{1/2})\Bigg\{ \\ &\quad - 1/4(1-\eta)u_2 - 1/4(1+\eta)u_3 + 1/2(1-\eta)u_5 + 1/2(1+\eta)u_7\Bigg\} \\ &\quad - 1/4\eta(1-\eta)u_2 + 1/4\eta(1+\eta)u_3 + 1/2(1-\eta^2)u_6\Bigg] \end{aligned}$$

(For Quadrilateral Element) (28)

with

$$\eta = \frac{\tan(\theta-\alpha/2)}{\tan(\alpha/2)} \quad . \tag{29}$$

and

$$u = \frac{r^{1/2}}{\{2\sin\alpha\ \sin\alpha/2\ \cos(\theta-\alpha/2)\}^{1/2}}\Big[-(u_2+4u_4)\sin(\alpha-\theta) - (u_3+4u_6)\sin\theta\Big] + O(r)$$

(For Triangular Elements) (30)

THE THREE-DIMENSIONAL CASE

The three-dimensional twenty-node isoparametric quadratic 'Brick' element is formulated in much the same way, by mapping the geometry into curvilinear space (ξ,η,ζ) of a normalized cube $(-1 \leq \xi, \eta, \zeta \leq 1)$ by the quadratic shape function [9],

$$x = \sum_{i=1}^{20} N_i(\xi,\eta,\zeta)x_i \ ,$$

$$y = \sum_{i=1}^{20} N_i(\xi,\eta,\zeta)y_i \ ,$$

$$z = \sum_{i=1}^{20} N_i(\xi,\eta,\zeta)z_i \ , \tag{31}$$

$$\begin{aligned} N_i = {} & 1/8(1+\xi\xi_i)(1+\eta\eta_i)(1+\zeta\zeta_i)(\xi\xi_i + \eta\eta_i + \zeta\zeta_i - 2)\,\xi_i^2\,\eta_i^2\,\zeta_i^2 \\ & + 1/4(1-\xi^2)(1+\eta\eta_i)(1+\zeta\zeta_i)(1-\xi_i^2) \\ & + 1/4(1-\eta^2)(1+\xi\xi_i)(1+\zeta\zeta_i)(1-\eta_i^2) \\ & + 1/4(1-\zeta^2)(1+\xi\xi_i)(1+\eta\eta_i)(1-\zeta_i^2) \ , \end{aligned}$$

where N_i is the shape function at node i (i = 1 to 20) whose Cartesian and curvilinear coordinates are (x_i, y_i, z_i) and (ξ_i, η_i, ζ_i) respectively. It should be noted that the shape function given in Equation (31) is obtained by superposition of those given in [9]. The geometry of the unit cube and the numbering sequence is shown in Figure 4.

For the isoparametric formulation, the displacements are given by

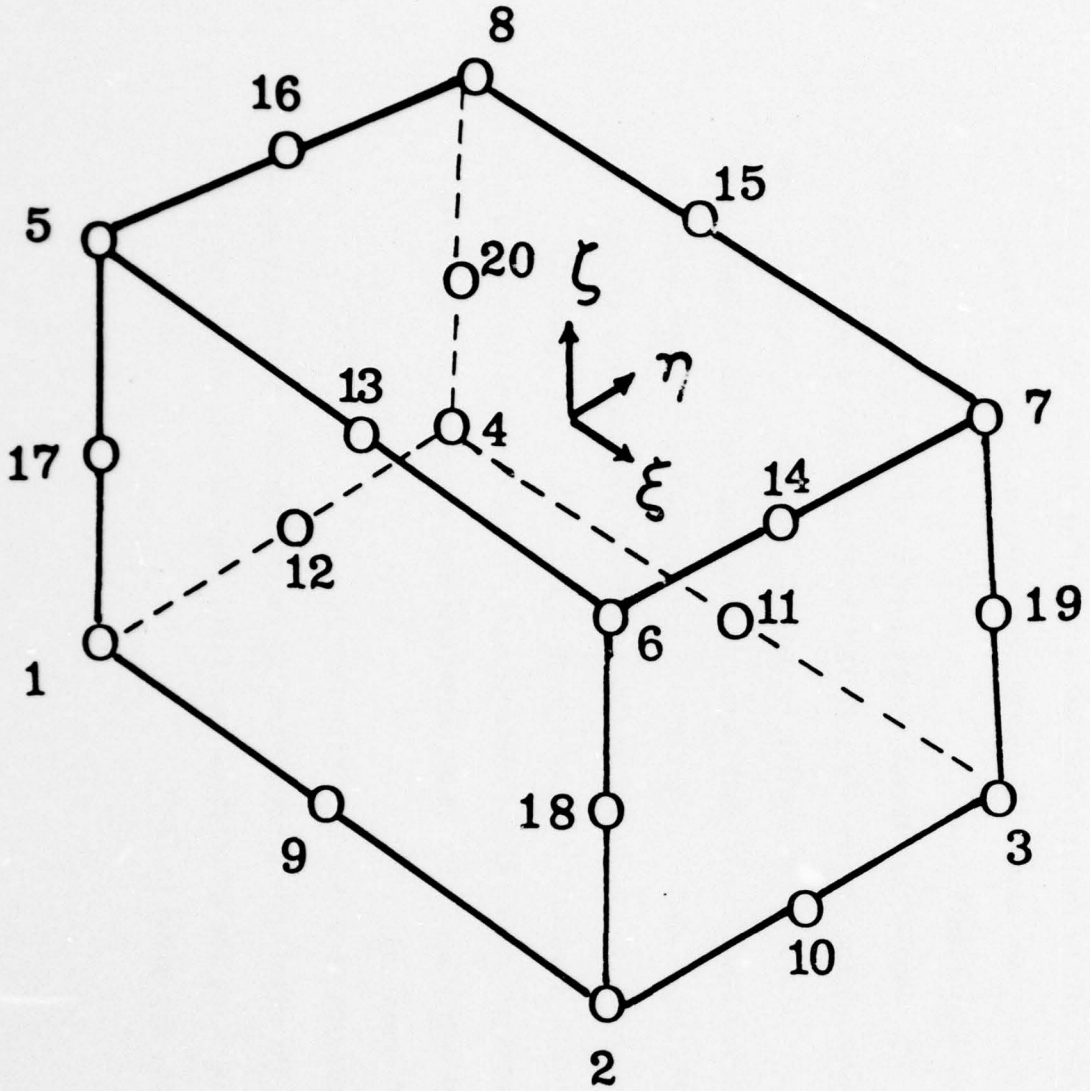

Figure 4. Numbering sequence of an isoparametric, quadratic, 'brick' element.

$$u = \sum_{i=1}^{20} N_i(\xi,\eta,\zeta)u_i \ ,$$

$$v = \sum_{i=1}^{20} N_i(\xi,\eta,\zeta)v_i \ , \qquad (32)$$

$$w = \sum_{i=1}^{20} N_i(\xi,\eta,\zeta)w_i \ .$$

The rest of the analysis follows in a similar fashion that given for the two-dimensional cases with appropriate augmentation to the three-dimensional quantities.

The singularity element is obtained by collapsing one face, 2376, and placing the midside nodes 9, 13, 11, 15 of Figure 4 at quarter points. The singular element is shown in Figure 5, in Cartesian coordinates. Since the elements are isoparametric they automatically satisfy inter-element compatibility and continuity in their regular or singular forms. It should be noted that the displacements are not singular. Further, it is easily shown that $\sum_i N_i = 1$. Hence, by theorems given in [9] the elements satisfy the constant strain and rigid body modes. The above conditions are necessary for the "patch test" mentioned in [2].

COMPUTATION OF STRESS INTENSITY FACTORS

The mixed mode stress intensity factors can be computed at quarter points using the Westergaard near field displacements which, for plane stress, are given in [10].

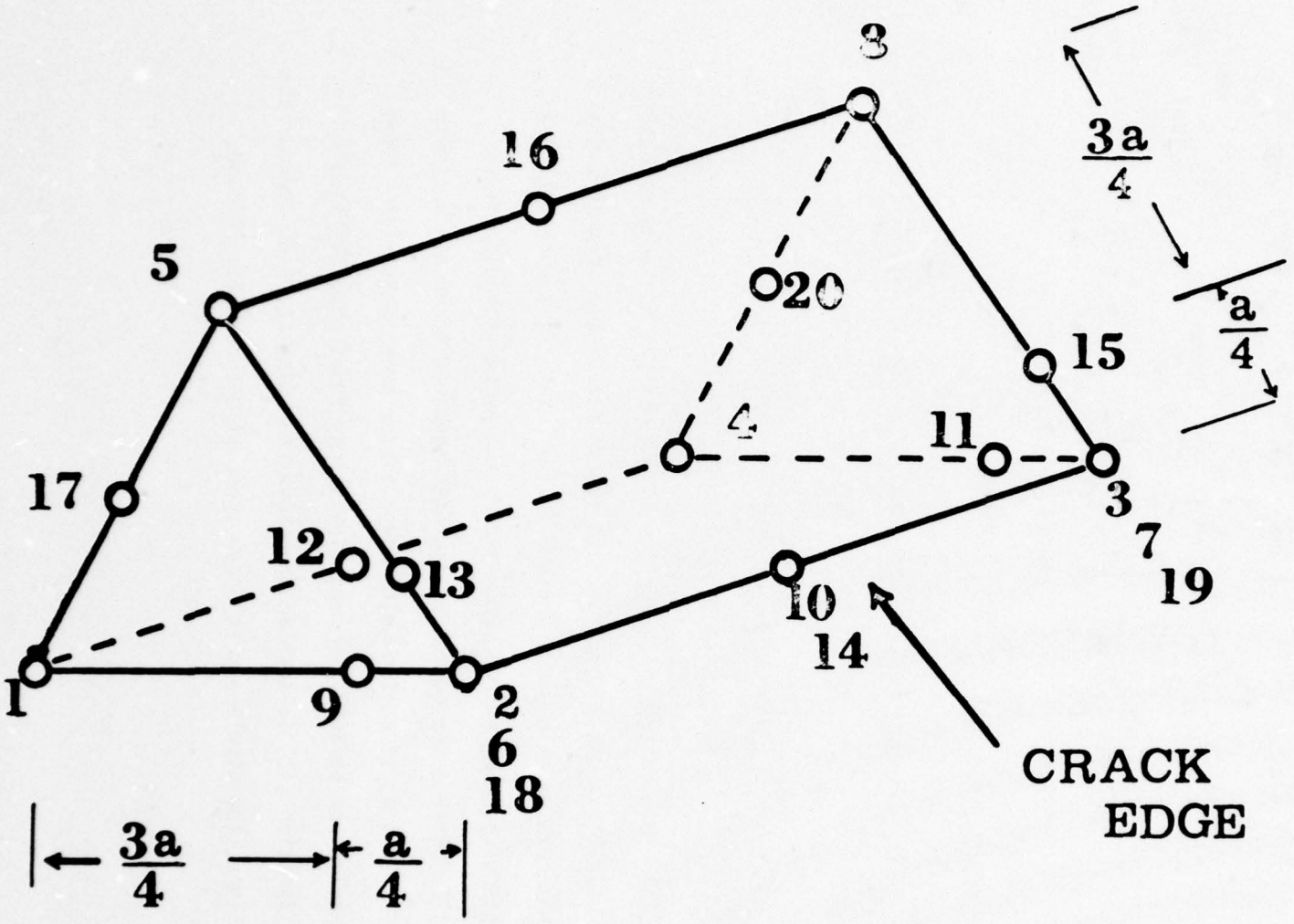

Figure 5. Singularity element obtained by collapsing the face 2376 and placing the nodes 9, 13, 11, and 15 at quarter points.

$$u = \frac{K_I}{G}\left(\frac{r}{2\pi}\right)^{1/2} \cos\theta/2 \left[\frac{1-\nu}{1+\nu} + \sin^2\theta/2\right] + \frac{K_{II}}{G}\left(\frac{r}{2\pi}\right)^{1/2} \sin\theta/2 \left[\frac{2}{1+\nu} + \cos^2\theta/2\right]$$

$$v = \frac{K_I}{G}\left(\frac{r}{2\pi}\right)^{1/2} \sin\theta/2 \left[\frac{2}{1+\nu} - \cos^2\theta/2\right] + \frac{K_{II}}{G}\left(\frac{r}{2\pi}\right)^{1/2} \cos\theta/2 \left[-\frac{1-\nu}{1+\nu} + \sin^2\theta/2\right] \quad (33)$$

Solving for K_I, K_{II} we have:

$$K_I = G\left(\frac{2\pi}{r}\right)^{1/2} \frac{u \cos\theta/2 \left[-\frac{2\nu}{1+\nu} + \cos^2\theta/2\right] + v \sin\theta/2 \left[\frac{2}{1+\nu} + \cos^2\theta/2\right]}{\left[\frac{2}{1+\nu} - \cos^2\theta/2\right]\left[\frac{2}{1+\nu} - \cos^2\theta/2\right]}$$

$$K_{II} = G\left(\frac{2\pi}{r}\right)^{1/2} \frac{u \sin\theta/2 - v \cos\theta/2}{\left[\frac{2}{1+\nu} - \cos^2\theta/2\right]} \quad (34)$$

It should be noted that Equation (33) is only a one-term expansion of the near field crack solution. To obtain reasonable accuracy, the quarter points have to be very close to the crack tip even though the elements surrounding such a crack embody the proper singular field. This will increase the number of elements required to obtain accurate results. Thus it is advisable to use a higher order expansion. Such an expansion can be obtained from airy stress functions. William's stress function [11] is such an expansion and using it, with appropriate corrections, the displacements under plane stress condition become,

$$2Gu = \sum_{n=1,2,3}^{\infty} \Bigg\{ (-1)^{n-1} d_{2n-1} \Bigg[(n-1/2)\cos(n-5/2)\theta - \left(\frac{3-\nu}{1+\nu} + n - \frac{3}{2}\right) \cos(n-1/2)\theta \Bigg] r^{n-1/2}$$

$$(-1)^{n} d_{2n} \left[n \cos(n-2)\theta - \left(\frac{3-\nu}{1+\nu} + n + 1\right) \cos n\theta \right] r^{n}$$

$$(-1)^{n-1} a_{2n-1} \left[(n-1/2)\sin(n-5/2)\theta - \left(\frac{3-\nu}{1+\nu} + n + 1/2\right) \sin(n-1/2)\theta \right] r^{n-1/2}$$

$$(-1)^{n} a_{2n} \left[n \sin(n-2)\theta - \left(\frac{3-\nu}{1+\nu} + n - 1\right) \sin n\theta \right] r^{n} \Bigg\} \qquad (35)$$

$$2Gv = \sum_{n=1,2,..}^{\infty} \Bigg\{ (-1)^{n-1} d_{2n-1} \Bigg[-(n-1/2)\sin(n-5/2)\theta - \left(\frac{3-\nu}{1+\nu} - n + 3/2\right) \sin(n-1/2)\theta \Bigg] r^{n-1/2}$$

$$(-1)^{n} d_{2n} \left[-n \sin(n-2)\theta - \left(\frac{3-\nu}{1+\nu} - n - 1\right) \sin n\theta \right] r^{n}$$

$$(-1)^{n-1} a_{2n-1} \left[(n-1/2)\cos(n-5/2)\theta + \left(\frac{3-\nu}{1+\nu} - n - 1/2\right) \cos(n-1/2)\theta \right] r^{n-1/2}$$

$$(-1)^{n} a_{2n} \left[n\cos(n-2)\theta + \left(\frac{3-\nu}{1+\nu} - n + 1\right) \cos n\theta \right] r^{n} \qquad (36)$$

Comparing with the Westergaard's solution we obtain

$$K_I = -\sqrt{2\pi}d_1$$
$$K_{II} = -\sqrt{2\pi}a_1 \qquad (37)$$

NASTRAN IMPLEMENTATION

The isoparametric quadratic quadrilateral, triangular and brick elements have been implemented using the NASTRAN dummy user element facility as outlined in Section 6.8.5 of [12]. This involved coding element stiffness and stress data recovery subroutines using the analysis outlined above and relinking the affected NASTRAN Links. Additional modifications were required to some of the Output File Processor (OFP) routines. These changes are detailed below.

The quadrilateral element was implemented as a DUM1 element. KDUM1, the element stiffness matrix subroutine, obtains material and grid point information from the element connection and property table (ECPT) and builds the matrices required to perform the integration in Equation (10). The integration is performed numerically using compound 3-point Gaussian quadrature as explained in [9]. This results in 9 evaluations of the integrand. Once the 16 by 16 stiffness matrix is complete, the appropriate 2 by 2 submatrices corresponding to the given pivot point are entered into the upper left of the 6 by 6 submatrices required by SMA1B, the stiffness matrix insertion subroutine. SMA1B is called 8 times for each pivot point. The time for element stiffness generation is 6 seconds per element on an IBM 360 Model 44.

NASTRAN stress data recovery is accomplished in two phases. During phase I, SDUM11 calculates [D][B] from Equations (5) and (9) for each grid point and passes the resultant 24 by 16 matrix to SDUM12 for final stress calculations. SDUM11 also checks for singularities in the inverse of the Jacobian [Equation (7)] and flags those grid points which have a singularity. Information passed to SDUM12 from SDUM11 includes the element id, grid point numbers, grid point singularity flag, coordinates of the eight grid points, crack orientation angle and the material constants E, G and ν. SDUM12, phase II of the stress recovery, locates the displacements associated with a given element and multiplies [D][B] times these displacements [Equation (4) and (8)] to give the stress components at each of the eight grid points. Grid point flags are checked for singular grid points and, if singularities exist, Mode I and Mode II stress intensity factors are calculated using Equations (35) and (36) with a two term expansion. These stress intensity factors at the quarter points are output at the mid-side node of the collapsed side while the corresponding corner node stress outputs are set to zero. The point ids of the singular corner nodes are negated and the mid-side id is set to overflow the integer field specification, thus flagging the point with asterisks.

OFP has been modified to output the eight sets of stress components for each element. These modifications were implemented by adding heading formats to OFPIA and changing the appropriate pointers and format specifications in OFP1BD, OFP5BD and OF1PBD. Although the ADUM cards allow sufficient flexibility to implement the element stiffness subroutine,

changes were required to GPTAL which describes the connection and property characteristics of each element. (See Section 2.5.2.1 in [12].) These changes were required to handle the expanded stress requirements. The number of words SDR2 passes from phase I to phase II was changed from 100 to 430 while the count of words SDR2 outputs for real stresses was increased from 10 to 33.

The triangular element was implemented in a similar fashion to the quadrilateral. In this case a DUM3 element was defined and appropriate KDUM3, SDUM31 and SDUM32 routines were written adhering to the analysis defined in an earlier section. Numerical integration was performed in KDUM3 using 6 point Hammer quadrature [9].

The implementation of the twenty node brick element was not as straightforward as that of the quadrilateral element. The brick was implemented as a DUM2 element. DIMENSION changes were required in TA1A and TA1B since NASTRAN assumes a maximum of 10 grid points per element. KDUM2 was initially implemented similarly to KDUM1. However, in this case, the integration using a 3-point Gaussian quadrature requires 27 integrand evaluations with a stiffness matrix of order 60. The size of the KDUM2 subroutine necessitated a change to the overlay structure of LINK3, placing KDUM2 in its own overlay segment. Also, since NASTRAN calls the stiffness routines based upon the pivot point concept, the same brick element stiffness matrix is built twenty times in an analysis. This technique resulted in a 20 minute stay in SMA1 for a one element problem on an IBM 360 Model 44.

KDUM2 was rewritten to build only the requested submatrices, i.e. those corresponding to the pivot point. Also, the matrix product

B^TDB (Equation 10) was performed explicitly, taking advantage of zero entries in the B and D matrices (Equations 5 and 9). These changes resulted in a reduction of computer time to 2 minutes per element in SMA1.

Stress data recovery is also nonstandard for the brick element. Due to the size of the arrays used in stress recovery for the brick, phase I has a limited function of assembling arrays dependent on parameters not available to phase II. The majority of calculations for stress recovery are accomplished during phase II, saving storage but increasing stress recovery times. Quantities passed from phase I to phase II are the stress-strain matrix [D], the element id, grid point ids, grid point coordinates and the material constants E, G, and ν. Phase II locates the displacements, calculates the stress components for each grid point, checks for singular Jacobians and calculates stress intensity factors as required. Stress intensity factors are displayed in a manner similar to that employed for the quadrilateral element.

OFP has been modified to output the twenty sets of stress components for each element. A DIMENSION change was also required in OFP to allow twenty grid points per element. OFP1A, OFP1BD, OFP5BD and OF1PBD were updated to produce the required heading and output formats. GPTAL was changed to increase the number of words to 120 that SDR2 passes from phase I to phase II. The count of words SDR2 outputs for real stresses was increased to 141.

The three element implementations were checked independent of

NASTRAN via dummy driver routines for SMA1 and SDR2. The coding for the element stiffness subroutines was verified by multiplying the stiffness matrix for one element times the known displacements for a uniform stress field. The resultant nodal loading was compared to that found analytically from (for the two-dimensional case)

$$\{F\}^e = \int_{-1}^{1}\int_{-1}^{1} [B]^T \{\sigma\} \, d\xi \, d\eta \qquad (38)$$

Figure 6 illustrates equivalent nodal forces for $\sigma_y = 1$ on the normalized square ($-1 \leq x,y \leq 1$). The stress recovery coding was checked by passing the known displacements for a uniform stress field to the stress recovery subroutines and observing the constant stress results.

The appendix describes the formats for each of the bulk data cards.

A FEW NUMERICAL RESULTS

To assess the accuracy of the method, three test problems with a fairly coarse grid (68 elements and approximately 239 grid points) were run. The problems are the single edge crack, double edge crack and center crack. These three problems can be done in a single run as subcases with different single point constraints as shown in Figure 7a, b, and c. The solutions of the above problems, by various methods, have been well documented [13]. Using quadrilaterial elements, it was found that the finite element solutions were accurate to within 2-3%. Graphically, this is illustrated in Figure 8 for the double edge crack by using the Westergaard near field solution [10] for σ_y.

ASTM has stringent requirements for the size of specimens for fracture toughness testing. However, in many applications of

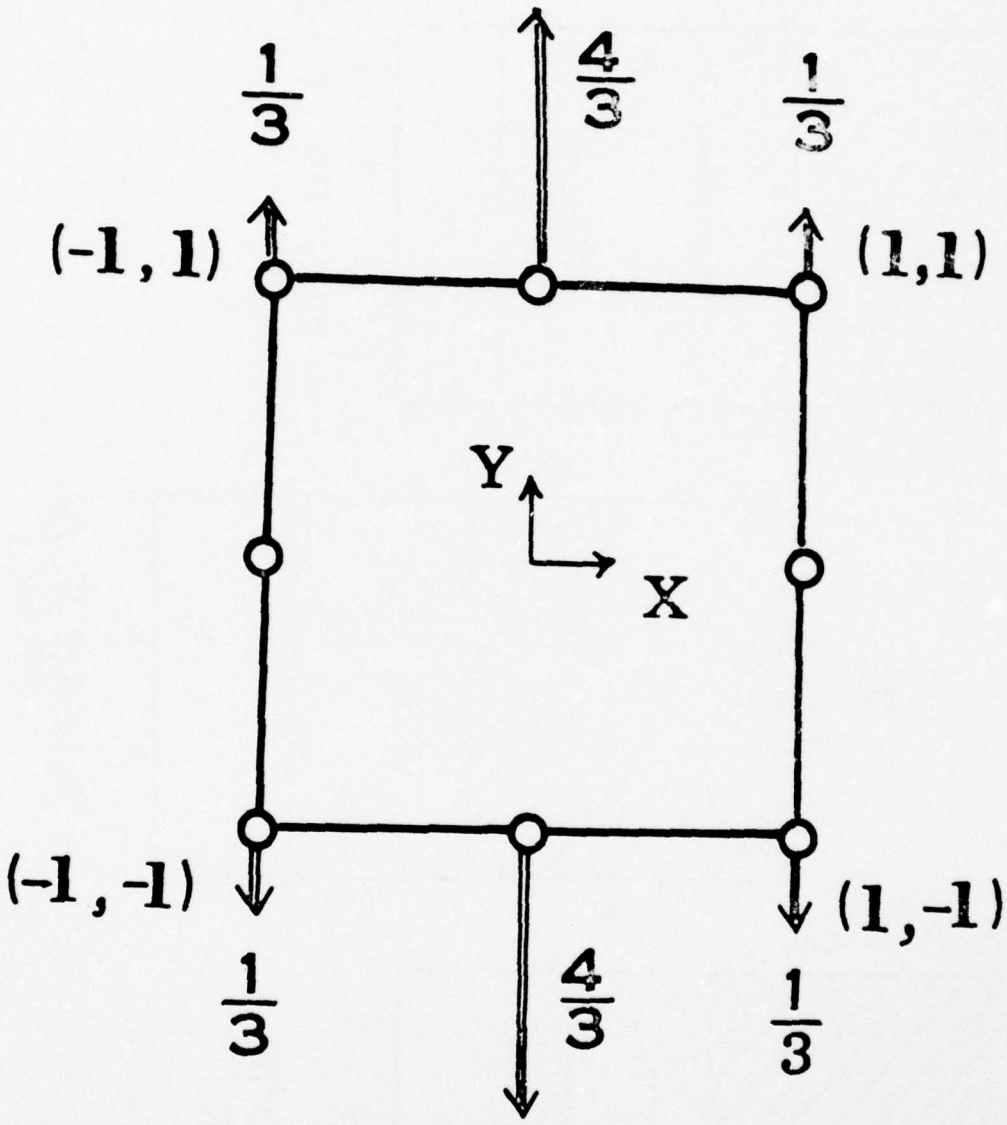

Figure 6. Equivalent nodal forces required for σ_y=1.

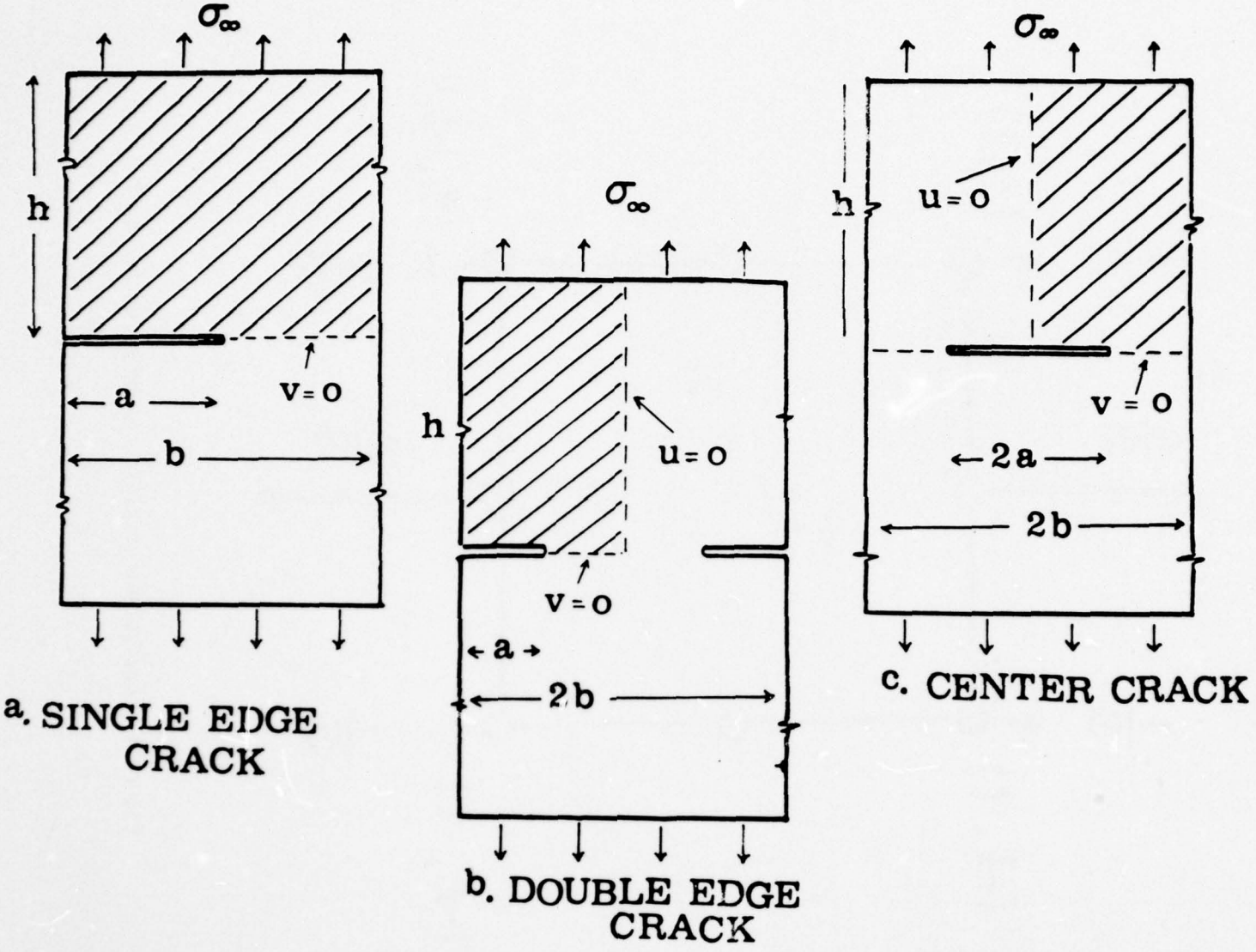

Figure 7. Test problem: shaded area analysed by finite elements. ($\frac{a}{b}=\frac{1}{2}, \frac{h}{b}=4$)

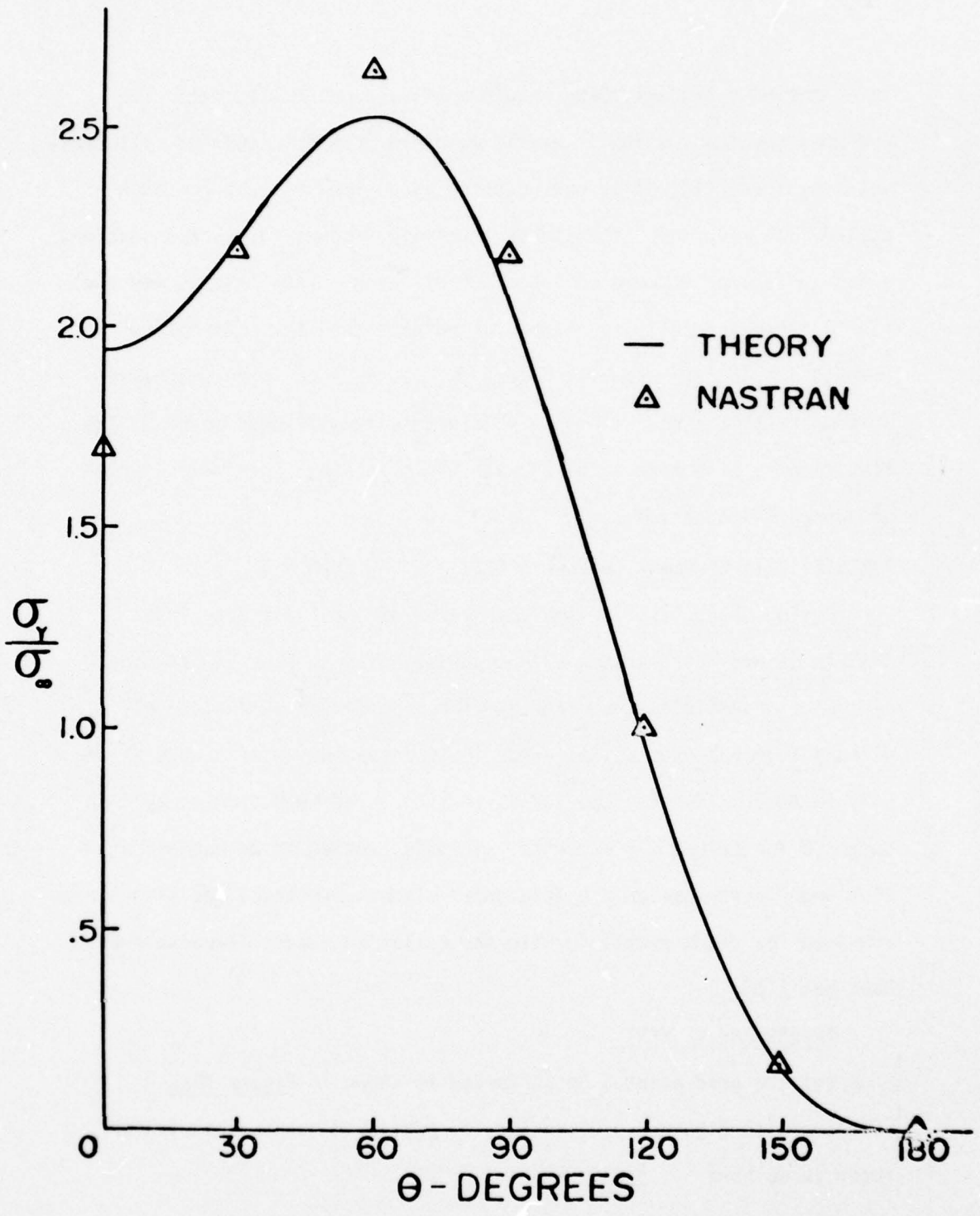

Figure 8. Comparison of NASTRAN results with the theoretical solution for a double-edge crack.

thick-walled cylinders these requirements are not easily met. The C-shaped specimen, which is easily obtained from thick-walled cylinders, was suggested [14] and is now accepted as a standard test for such cylindrical material. The stress intensity factors for such a section, shown in Figure 9, were computed for different crack lengths and the finite element results, experimental results, and the collocation results of [15] are shown in Figure 9 . It is seen that remarkable agreement is obtained with just 48 elements and 171 grid points. The results have also been compared with those in [16] and similar correspondence was observed.

THE STABILITY OF QUADRILATERAL AND TRIANGULAR ELEMENTS

During the process of implementation of these elements into NASTRAN it was found that a slight perturbation in placing the mid-side node opposite to the crack tip for a collapsed quadrilateral element led to a substantial error in the computation of stress intensity factors. (See the Conclusion in [18].) No such errors could be detected for triangular elements. In this section it is demonstrated that under perturbation the triangular element preserves the singularity required for crack problems while the collapsed quadrilateral element does not [19].

TRIANGULAR ELEMENT

Let the grid point 5 be perturbed as shown in Figure 10a. (Compare with Figure 3.) Denoting the perturbed quantities with an asterisk we have

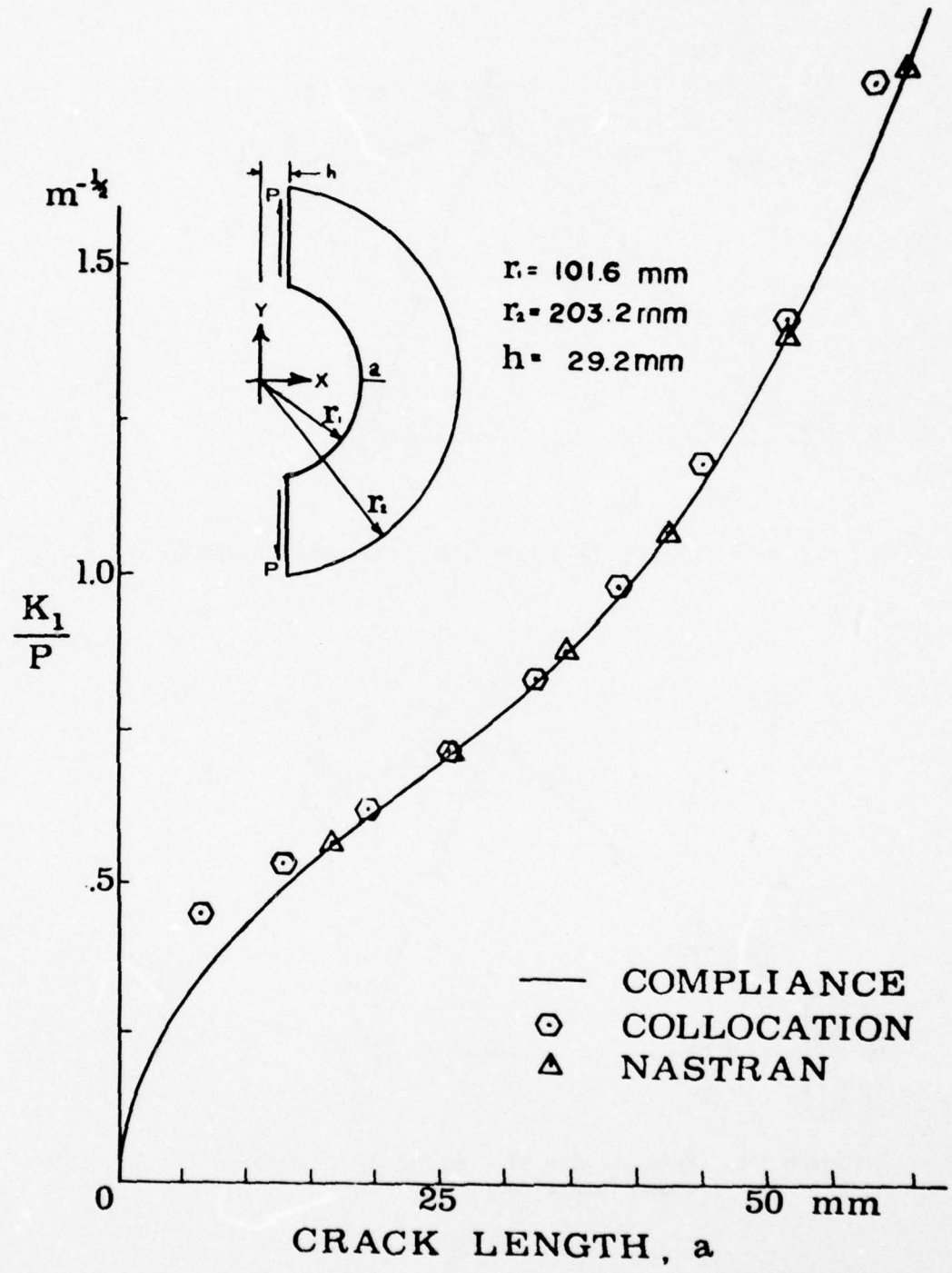

Figure 9. Comparison of NASTRAN results with those obtained experimentally and by collocation.

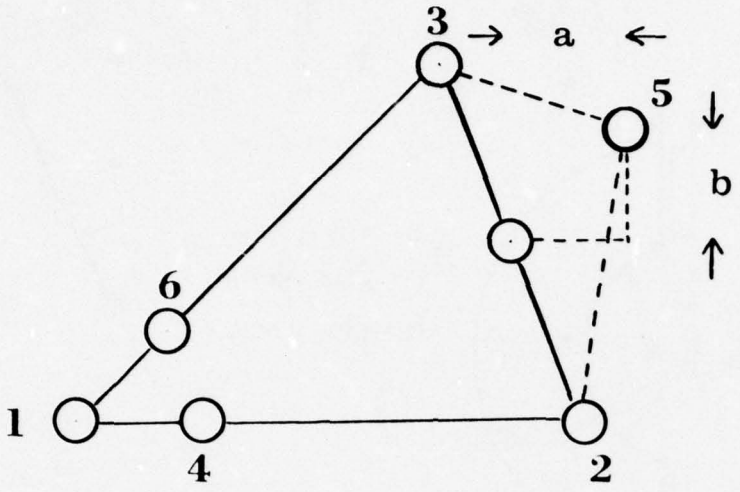

Figure 10a. Perturbation of a singular, triangular element.

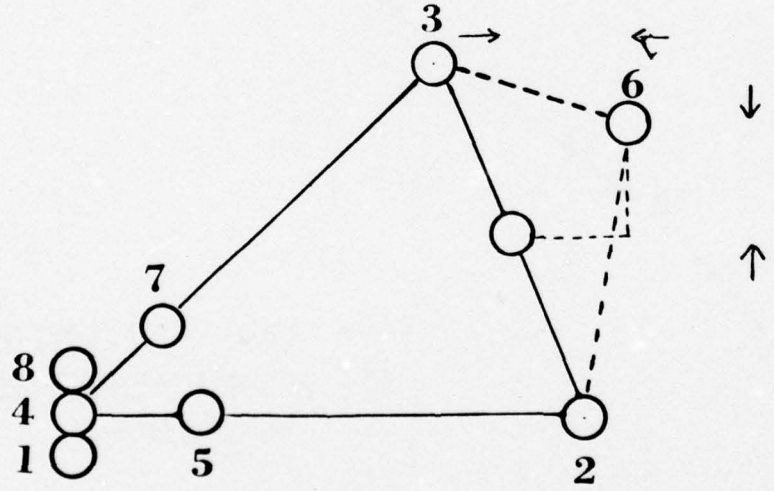

Figure 10b. Perturbation of a collapsed singular, quadrilateral element.

$$x_5^* = \cos^2\frac{\alpha}{2} + a$$

$$y_5^* = \sin\frac{\alpha}{2}\cos\frac{\alpha}{2} + b \qquad \text{For Grid Point 5} \tag{39}$$

We have

$$\text{Det}|J^*| = \text{Det}|J| - (8L_3^2\sin\alpha)a - (8L_3^2\cos\alpha - 4L_2^2)b \tag{40}$$

As seen the perturbed Jacobian vanishes at grid point 1 ($L_1 = 1$, $L_2 = L_3 = 0$) for all values of perturbation parameters a and b. The order of singularity, however, will only become apparent when we look at the coordinate transformation

$$x^* = \sum_{i=1}^{6} N_i x_i = x + aN_5 \tag{41}$$

$$= (L_2 + L_3)[L_2 + L_3\cos\alpha] + 4aL_2L_3$$

$$y^* = \sum_{i=1}^{6} N_i y_i = y + bN_5 \tag{42}$$

$$= (L_2 + L_3)L_3\sin\alpha + 4bL_2L_3$$

Solving for L_3 we have

$$L_3^2 = \frac{(By^* + cx^*) \pm \sqrt{(By^* + cx^*)^2 - 4Ay^{*2}}}{2A} \tag{43}$$

where

$$A = -4a\sin^2\alpha - 4b\sin\alpha(1-\cos\alpha) - 16ab\sin\alpha + 16b^2\cos\alpha$$

$$B = 2\sin\alpha - (4b + \sin\alpha)(1 + 4a + \cos\alpha) \tag{44}$$

$$C = (4b + \sin\alpha)^2$$

Using the polar coordinates ($x^* = r\cos\theta$, $y^* = r\sin\theta$) we have from (43)

$$L_3 = r^{1/2}\left[\frac{(B\sin\theta + C\cos\theta) \pm \sqrt{(B\sin\theta + C\cos\theta)^2 - 4A\sin^2\theta}}{2A}\right]^{1/2} \quad (45)$$

with a similar expression for L_2. Comparing Equation (45) with the unperturbed case [Equation (27)] we see that L_2, L_3 and consequently the displacements have the same behavior as the unperturbed case. Hence for the case of the triangular element, the singularity is preserved under perturbation.

QUADRILATERAL CASE

Let grid point 6 be perturbed as shown in Figure 10b. For simplicity let $a = b = \varepsilon$. (It is sufficient to show the lack of singularity on one ray.) Then

$$x^* = \frac{1}{8}(1+\xi)^2\left[(1+\cos\alpha) - \eta(1-\cos\alpha)\right] + \frac{\varepsilon}{2}(1-\eta^2)(1+\xi) \quad (46)$$

$$y^* = \frac{1}{8}\sin\alpha(1+\xi)^2(1+\eta) + \frac{\varepsilon}{2}(1-\eta^2)(1+\xi) \quad (47)$$

Along the line $x^* = y^*$ we have from (46) and (47),

$$\eta = \frac{1 + \cos\alpha - \sin\alpha}{1 - \cos\alpha + \sin\alpha} = \text{constant} = c \quad \text{(SAY)}$$

Substituting η into Equation (47) and solving we have (in terms of polar coordinates, $x^* = y^* = r\sin\theta$, $\theta = \pi/4$)

$$(1+\xi) = \frac{\varepsilon(c^2-1)}{\sin\alpha(1+c)}\left[1 - \sqrt{1 + \frac{2\sin\alpha(1+c)}{\varepsilon^2(c^2-1)^2}\, r\sin\theta}\right] \quad (48)$$

Since $(1+\xi)$ is the common factor in the displacement (28) it is seen that there is at least one ray in the collapsed quadrilateral case where the singularity required for the crack problems disappears. Hence such

perturbations of the collapsed quadrilateral elements, which may either be caused by automatic mesh generation or simply by transcription errors may lead to unstable answers.

NUMERICAL RESULTS FOR STABILITY

To illustrate the effect of perturbing the mid-side node let us consider a crack of length 2a in an infinite media under a uniform tension of P applied normal to the crack. The solution of the problem is well known. Using Muskhelishvili's method [17], we have for the plane stress condition displacements given by

$$u + iv = \frac{(1+\nu)}{E}\left[\frac{(3-\nu)}{(1+\nu)}\phi(z) - z\,\overline{\phi(z)} - \overline{\psi(z)}\right] \tag{49}$$

where

$$\phi(z) = \frac{Pa}{8}\left[\frac{z}{a} + \left(\frac{z^2}{a^2} - 1\right)^{1/2} - \frac{3}{\frac{z}{a} + \left(\frac{z^2}{a^2} - 1\right)^{1/2}}\right]$$

$$\phi(z) = \frac{P}{4}\left[\frac{2\,z/a}{\left(\frac{z^2}{a^2} - 1\right)^{1/2}} - 1\right] \tag{50}$$

$$\psi(z) = \frac{Pa}{4}\left[2\left(\frac{z^2}{a^2} - 1\right)^{1/2} - \frac{1}{\left(\frac{z^2}{a^2} - 1\right)^{1/2}} - \frac{1}{\left(\frac{z^2}{a^2} - 1\right)^{1/2}\left\{\frac{z}{a} + \left(\frac{z^2}{a^2} - 1\right)^{1/2}\right\}^2}\right]$$

For a finite element grid of 12 elements as shown in Figure 11, the displacements computed from (49) were prescribed at corner grid points. The displacements were computed at quarter points using collapsed quadrilateral as well as triangular elements. The results obtained by both methods were in very close agreement with the theoretical results of (49). However when the opposite node of the 1st element was perturbed the results from the collapsed quadrilateral elements were quite unstable compared to those obtained from triangular elements. This is illustrated in Figure (12) with 0%, 20%, and 40% perturbation of a single opposite node of the 1st element. It was seen that the error is of the order $\frac{\Delta r}{r}$ for the quadrilateral case. There was no significant change in results for the case of triangular elements as seen in Figure 13.

CONCLUSIONS

Quadratic quadrilateral and triangular isoparametric elements can be easily used to construct an elastic singular element for analyzing crack problems. Collapsed quadrilateral elements are less stable in preserving the elastic singularity, under perturbation of the opposite mid-side nodes, than the triangular elements. These elements have been implemented in NASTRAN. Similar elements can be also constructed from cubic elements. The plastic singularity can also be achieved by the use of "sliding node" concepts. These questions will be investigated in the near future.

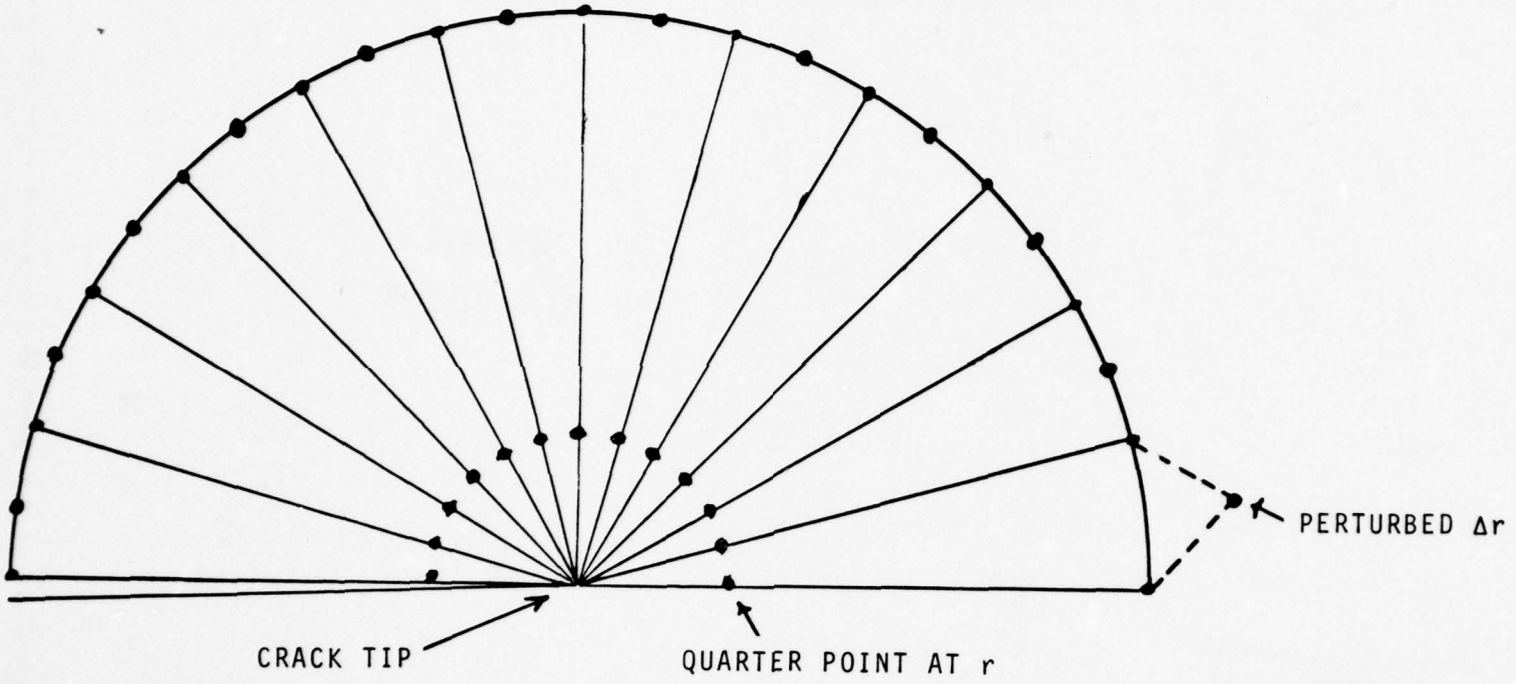

Figure 11. Finite element grid to test the effect of perturbation of a node, with displacements prescribed for all of the corner nodes.

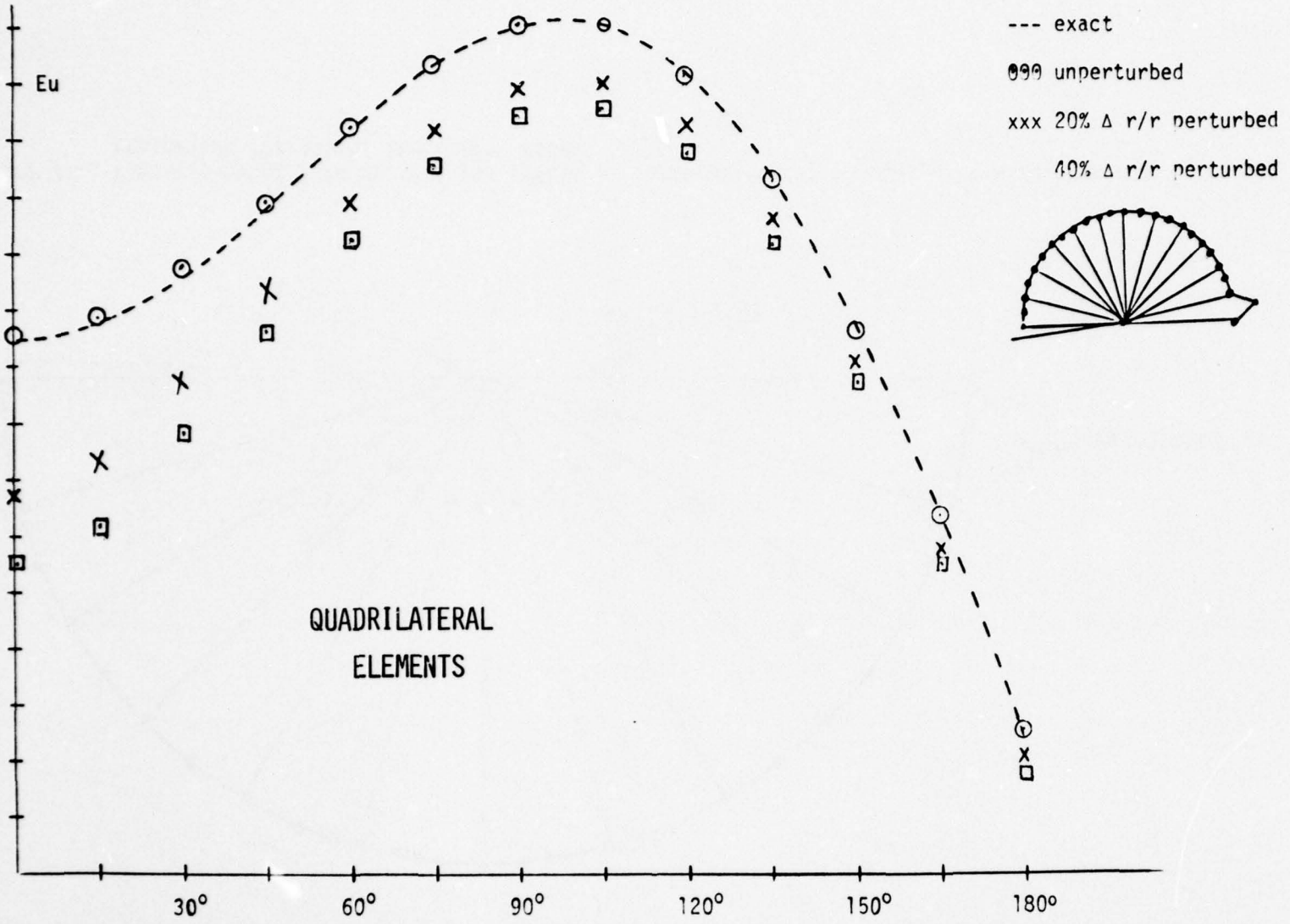

Figure 12. Displacements at quarter points from finite elements with displacements at corner points prescribed - the results indicate unstable behavior under perturbation.

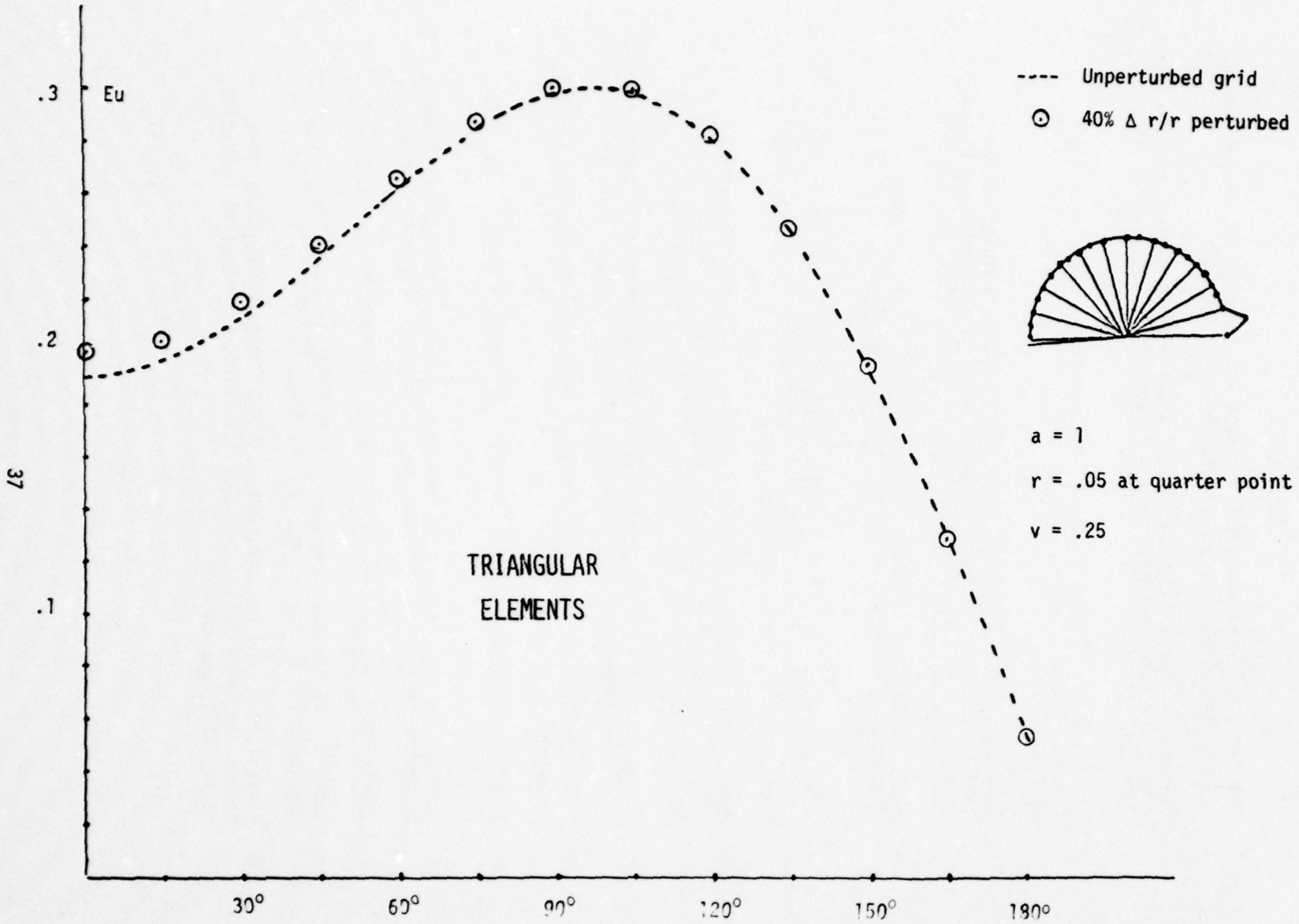

Figure 13. Displacements at quarter points from finite elements with displacements at corner points prescribed - the results indicate stability of triangular singular elements under perturbation.

REFERENCES

1. Henshell, R.D. and Shaw, K.G. "Crack Tip Elements are Unnecessary", Int. J. Num. Meth. Engrg, Vol. 9, 1975, pp. 495-507.

2. Barsoum, Roshdy S. "On the Use of Isoparametric Finite Elements in Linear Fracture Mechanics", Int. J. Num. Meth. Engrg., Vol. 10, 1976, pp. 25-76.

3. Tracey, D.M. "Finite Elements for Determination of Crack Tip Elastic Stress Intensity Factors", Eng. Fract. Mech., Vol. 3, 1971, pp. 255-265.

4. Wilkinson, R.F. and Kelley, J.W. "A Failsafe Analysis Using NASTRAN's Piecewise Linear Analysis and a Nine Node Linear Element", NASTRAN: Users' Experiences, NASA TM X-3278, 1975, pp. 181-200.

5. Aberson, J.A. and Anderson, J.M. "Cracked Finite Elements Proposed for NASTRAN", NASTRAN: Users' Experiences, NASA TM X-2893, 1973.

6. Anderson, G.P., Ruggles, V.L. and Stibor, G.S. "Use of Finite Element Computer Programs in Fracture Mechanics", Int. J. Fract. Mech., Vol. 7, March 1971, pp. 63-76.

7. Chan, S.K., Tuba, I.S. and Wilson, W.K. "On the Finite Element Method in Linear Fracture Mechanics", Eng. Fract. Mech., Vol. 2, No. 1, 1970, pp. 1-17.

8. McDonough, J.R. "A Survey of NASTRAN Improvements Since Level 15.5", NASTRAN: Users' Experiences, NASA TM X-3278, 1975, pp. 11-22.

9. Zienkiewicz, O.C. The Finite Element Method in Engineering Science, McGraw-Hill, London, 1971.

10. "Fracture Toughness Testing and Its Applications", ASTM, STP 381, pp. 32-33.

11. Williams, M. L. "Stress Distribution at Base of Stationary Crack", J. Applied Mechanics, Vol. 24, No. 1, pp. 109-114, March 1957.

12. The NASTRAN Programmer's Manual. NASA SP-223(01), Sep 1972.

13. Tada, H., Paris, C.P. and Irwin, G.R. The Stress Analysis of Cracks Handbook, Del Research Corporation, 1973, pp. 2.1-2.11.

14. Kendall, D.P. and Hussain, M.A. "A New Fracture-Toughness Test Method for Thick-Walled Cylinder Material", Experimental Mechanics, April, 1972, pp. 184-189.

15. Hussain, M.A., Lorensen, W.E., Kendall, D.P. and Pu, S.L. "A Modified Collocation Method for C-Shaped Specimens", Watervliet Arsenal Technical Report, R-WVT-X-6-73, 1973.

16. Gross, B. and Srawley, J.E. "Analysis of Radially Cracked Ring Segments Subject to Forces and Couples", NASA TM X-71842, 1976.

17. Muskhelishvili, N.I. Some Basic Problems of the Mathematical Theory of Elasticity, P. Nobrdhoff, Ltd. Grovingen - The Netherlands, 1963, p. 508.

18. Hussain, M.A., Lorensen, W.E. and Pflegl, G. "The Quarter-Point Quadratic Isoparametric Element as a Singular Element for Crack Problems", NASTRAN: Users' Experiences, NASA TM X-3428, 1976.

19. Lorensen, W.E., Hussain, M.A. "The Stability of Isoparametric Triangular Elements As A Singular Element For Crack Problems", Developments in Mechanics, Vol. 8 - Proceedings of the 15th Midwestern Mechanics Conference, 1977. (Editor: T.C.T. Ting).

APPENDIX

BULK DATA DECKS

BULK DATA DECK

Input Data Card ADUM1

Description: Defines attributes for an isoparametric, quadratic quadrilateral implemented as a DUM1 dummy user element.

Format and Example:

ADUM1	NG	NC	NP	ND
ADUM1	8	0	1	3

Field	Contents
NG	Number of grid points connected by DUM1 (Integer = 8)
NC	Number of additional entries on CDUM1 (Integer = 0)
NP	Number of additional entries on PDUM1 (Integer = 1)
ND	Number of displacement components at each grid point used in generation of differential stiffness (Integer = 3)

Remarks:

1. All fields must correspond to the example.
2. One ADUM1 must be present if any CDUM1's are present.

BULK DATA DECK

Input Data Card ADUM3

Description: Defines attributes for an isoparametric, quadratic triangle implemented as a DUM3 dummy user element.

Format and Example:

ADUM3	NG	NC	NP	ND
ADUM3	6	0	1	3

Field	Contents
NG	Number of grid points connected by DUM3 (Integer = 6)
NC	Number of additional entries on CDUM3 (Integer = 0)
NP	Number of additional entries on PDUM3 (Integer = 1)
ND	Number of displacement components at each grid point used in generation of differential stiffness (Integer = 3)

Remarks:

1. All fields must correspond to the example.
2. One ADUM3 must be present if any CDUM3's are present.

BULK DATA DECK

Input Data Card ADUM2

Description: Defines attributes for an isoparametric, quadratic brick implemented as a DUM2 dummy user element.

Format and Example:

ADUM2	NG	NC	NP	ND
ADUM2	20	0	1	3

Field	Contents
NG	Number of grid points connected by DUM2 (Integer = 20)
NC	Number of additional entries on CDUM2 (Integer = 0)
NP	Number of additional entries on PDUM2 (Integer = 1)
ND	Number of displacement components at each grid point used in generation of differential stiffness (Integer = 3)

Remarks:

1. All fields must correspond to the example.
2. One ADUM2 must be present if any CDUM2's are present.

BULK DATA DECK

Input Data Card CDUM1

Description: Defines an isoparametric, quadratic, quadrilateral element (DUM1)

Format and Example:

CDUM1	EID	PID	C1	C2	C3	C4	M1	M2	+abc
CDUM1	25	14	1	2	3	4	5	6	ABC

+abc	M3	M4
+BC	7	8

Field	Contents
EID	Element identification number (Integer > 0)
PID	Identification number of a PDUM1 property card (Integer > 0)
C1,..,C4	Grid point identification numbers of corner points (Integers > 0, C1 ≠ C2 ≠ C3 ≠ C4)
M1,..,M4	Grid point identification numbers of 'mid-side' points (Integers > 0, M1 ≠ M2 ≠ M3 ≠ M4)

Remarks:

1. The order of the grid points is: C1, C2, C3, C4 counterclockwise; M1 is between C1 and C2, followed by M2, M3, M4.
2. The quadrilateral must lie wholly in the X-Y plane.
3. Stresses are given in the global system. For collapsed elements, mode I and II stress intensities are output.
4. If one side is collapsed to form a crack element, these rules must be followed:
   a. Sides adjacent to the collapsed side must be straight and have their 'mid-side' nodes located exactly 1/4 of the length of the side from the collapsed side.

b. The side opposite the collapsed side must be straight and have its 'mid-side' node located exactly 1/2 the distance between its corresponding corner nodes.

5. If degrees of freedom on the collapsed side are not constrained via single-point constraints, they should be constrained via multi-point constraints to maintain a physical correspondence (i.e., $U_1 = U_4 = U_8$, $V_1 = V_4 = V_8$).

BULK DATA DECK

Input Data Card CDUM2

Description: Defines an isoparametric, quadratic brick element (DUM2).

Format and Example:

CDUM2	EID	PID	C1	C2	C3	C4	C5	C6	+abc
CDUM2	31	7	1	2	3	4	5	6	ABC

+abc	C7	C8	M1	M2	M3	M4	M5	M6	+def
+BC	7	8	9	10	11	12	13	14	DEF

+def	M7	M8	M9	M10	M11	M12
+EF	15	16	17	18	19	20

Field	Contents
EID	Element identification number (Integer > 0)
PID	Identification number of a PDUM2 property card (Integer > 0)
C1,..,C8	Grid point identification of corner points (Integers > 0, C1 ≠...≠ C8)
M1,..,M12	Grid point identification numbers of 'mid-side' points (Integers > 0, M1 ≠... ≠ M12)

Remarks:

1. The order of the grid points is:
   C1, C2, C3, C4 about one face
   C5, C6, C7, C8 about the opposite face
   M1 is between C1 and C2, followed by M2, M3, M4
   M5 is between C5 and C6, followed by M6, M7, M8
   M9 is between C1 and C5, followed by M10, M11, M12.
2. Stresses are given in the global system. For collapsed bricks, mode I, II and III stress intensities are given.
3. For collapsed elements, the crack must lie wholly within some X-Y plane.
4. If one face is collapsed to form a crack element, these rules must be followed:
   a. Sides adjacent to the collapsed face must be straight and have their 'mid-side' nodes exactly 1/4 of the length of the side from the collapsed face.
   b. The line formed by the collapse of a face need not be straight.
5. If degrees of freedom on the collapsed side are not constrained via single-point constraints, they should be constrained via multi-point constraints to maintain physical correspondence (i.e., $U_1 = U_{17} = U_5$, $V_1 = V_{17} = V_5$, $W_1 = W_{17} = W_5$, $U_9 = U_{13}$, $V_9 = V_{13}$, etc.).

BULK DATA DECK

Input Data Card CDUM3

Description: Defines an isoparametric, quadratic, triangular element (DUM3)

Format and Example:

CDUM3	EID	PID	C1	C2	C3	M1	M2	M3
CDUM3	25	14	1	2	3	4	5	6

Field	Contents
EID	Element identification number (Integer > 0)
PID	Identification number of a PDUM1 property card (Integer > 0)
C1,C2,C3	Grid point identification numbers of corner points (Integers > 0, C1 ≠ C2 ≠ C3)
M1,M2,M3	Grid point identification numbers of 'mid-side' points (Integers > 0, M1 ≠ M2 ≠ M3)

Remarks:

1. The order of the grid points is: C1, C2, C3 counterclockwise; M1 is between C1 and C2, followed by M2, M3.
2. The triangle must lie wholly in the X-Y plane.
3. Stresses are given in the global system. For singular elements, mode I and II stress intensities are output.
4. To form a crack element, these rules must be followed:
   a. Sides adjacent to the crack tip must be straight and have their 'mid-side' nodes located exactly 1/4 of the length of the side from the crack tip.
   b. The side opposite the crack tip must be straight and have its 'mid-side' node located exactly 1/2 the distance between its corresponding corner nodes.

BULK DATA DECK

Input Data Card PDUM1

Description: Defines the properties of an isoparametric, quadratic, quadrilateral element. Referenced by a CDUM1 card.

Format and Example:

PDUM1	PID	MID	BETA
PDUM1	23	5	45.0

Field	Contents
PID	Property identification number
MID	Material identification number of a MAT1 card
BETA	Orientation angle in degrees of crack with respect to global system (Blank or real). BETA is positive for the top elements of the crack and negative for the bottom elements of the crack.

Remarks:

1. If BETA is blank, 0.0. is assumed.
2. BETA is only used for elements with a collapsed side. If specified for other elements, it is ignored.

BULK DATA DECK

Input Data Card PDUM2

Description: Defines the properties of an isoparametric, quadratic, brick element. Referenced by a CDUM2 card.

Format and Example:

PDUM2	PID	MID
PDUM2	75	1

Field	Contents
PID	Property identification number
MID	Material identification number of a MAT1 card

BULK DATA DECK

Input Data Card PDUM3

Description: Defines the properties of an isoparametric, quadratic, triangular element. Referenced by a CDUM3 card.

Format and Example:

PDUM3	PID	MID	BETA
PDUM3	23	5	45.0

Field	Contents
PID	Property identification number
MID	Material identification number of a MAT1 card
BETA	Orientation angle in degrees of crack with respect to global system (blank or real). BETA is positive for the top elements of the crack and negative for the bottom elements of the crack.

Remarks:

1. If BETA is blank, 0.0. is assumed.
2. BETA is only used for elements with a singularity. If specified for other elements, it is ignored.

WATERVLIET ARSENAL INTERNAL DISTRIBUTION LIST

May 1976

	No. of Copies
COMMANDER	1
DIRECTOR, BENET WEAPONS LABORATORY	1
DIRECTOR, DEVELOPMENT ENGINEERING DIRECTORATE	1
ATTN: RD-AT	1
RD-MR	1
RD-PE	1
RD-RM	1
RD-SE	1
RD-SP	1
DIRECTOR, ENGINEERING SUPPORT DIRECTORATE	1
DIRECTOR, RESEARCH DIRECTORATE	2
ATTN: RR-AM	1
RR-C	1
RR-ME	1
RR-PS	1
TECHNICAL LIBRARY	5
TECHNICAL PUBLICATIONS & EDITING BRANCH	2
DIRECTOR, OPERATIONS DIRECTORATE	1
DIRECTOR, PROCUREMENT DIRECTORATE	1
DIRECTOR, PRODUCT ASSURANCE DIRECTORATE	1
PATENT ADVISORS	1

EXTERNAL DISTRIBUTION LIST

December 1976

1 copy to each

OFC OF THE DIR. OF DEFENSE R&E
ATTN: ASST DIRECTOR MATERIALS
THE PENTAGON
WASHINGTON, D.C. 20315

CDR
US ARMY TANK-AUTMV COMD
ATTN: AMDTA-UL
AMSTA-RKM MAT LAB
WARREN, MICHIGAN 48090

CDR
PICATINNY ARSENAL
ATTN: SARPA-TS-S
SARPA-VP3 (PLASTICS
TECH EVAL CEN)
DOVER, NJ 07801

CDR
FRANKFORD ARSENAL
ATTN: SARFA
PHILADELPHIA, PA 19137

DIRECTOR
US ARMY BALLISTIC RSCH LABS
ATTN: AMXBR-LB
ABERDEEN PROVING GROUND
MARYLAND 21005

CDR
US ARMY RSCH OFC (DURHAM)
BOX CM, DUKE STATION
ATTN: RDRD-IPL
DURHAM, NC 27706

CDR
WEST POINT MIL ACADEMY
ATTN: CHMN, MECH ENGR DEPT
WEST POINT, NY 10996

CDR
HQ, US ARMY AVN SCH
ATTN: OFC OF THE LIBRARIAN
FT RUCKER, ALABAMA 36362

CDR
US ARMY ARMT COMD
ATTN: AMSAR-PPW-IR
AMSAR-RD
AMSAR-RDG
ROCK ISLAND, IL 61201

CDR
US ARMY ARMT COMD
FLD SVC DIV
ARMCOM ARMT SYS OFC
ATTN: AMSAR-ASF
ROCK ISLAND, IL 61201

CDR
US ARMY ELCT COMD
FT MONMOUTH, NJ 07703

CDR
REDSTONE ARSENAL
ATTN: AMSMI-RRS
AMSMI-RSM
ALABAMA 35809

CDR
ROCK ISLAND ARSENAL
ATTN: SARRI-RDD
ROCK ISLAND, IL 61202

CDR
US ARMY FGN SCIENCE & TECH CEN
ATTN: AMXST-SD
220 7TH STREET N.E.
CHARLOTTESVILLE, VA 22901

DIRECTOR
US ARMY PDN EQ. AGENCY
ATTN: AMXPE-MT
ROCK ISLAND, IL 61201

EXTERNAL DISTRIBUTION LIST (Cont)

1 copy to each

CDR
US NAVAL WPNS LAB
CHIEF, MAT SCIENCE DIV
ATTN: MR. D. MALYEVAC
DAHLGREN, VA 22448

DIRECTOR
NAVAL RSCH LAB
ATTN: DIR. MECH DIV
WASHINGTON, D.C. 20375

DIRECTOR
NAVAL RSCH LAB
CODE 26-27 (DOCU LIB.)
WASHINGTON, D.C. 20375

NASA SCIENTIFIC & TECH INFO FAC
PO BOX 8757, ATTN: ACQ BR
BALTIMORE/WASHINGTON INTL AIRPORT
MARYLAND 21240

DEFENSE METALS INFO CEN
BATTELLE INSTITUTE
505 KING AVE
COLUMBUS, OHIO 43201

MANUEL E. PRADO / G. STISSER
LAWRENCE LIVERMORE LAB
PO BOX 808
LIVERMORE, CA 94550

DR. ROBERT QUATTRONE
CHIEF, MAT BR
US ARMY R&S GROUP, EUR
BOX 65, FPO N.Y. 09510

2 copies to each

CDR
US ARMY MOB EQUIP RSCH & DEV COMD
ATTN: TECH DOCU CEN
FT BELVOIR, VA 22060

CDR
US ARMY MAT RSCH AGCY
ATTN: AMXMR - TECH INFO CEN
WATERTOWN, MASS 02172

CDR
WRIGHT-PATTERSON AFB
ATTN: AFML/MXA
OHIO 45433

CDR
REDSTONE ARSENAL
ATTN: DOCU & TECH INFO BR
ALABAMA 35809

12 copies

CDR
DEFENSE DOCU CEN
ATTN: DDC-TCA
CAMERON STATION
ALEXANDRIA, VA 22314

NOTE: PLEASE NOTIFY CDR, WATERVLIET ARSENAL, ATTN: SARWV-RT-TP, WATERVLIET, N.Y. 12189, IF ANY CHANGE IS REQUIRED TO THE ABOVE.